STEM EELS (Electron Energy-Loss Spectroscopy)

Odile Stéphan & Alexandre Gloter

STEM group
Laboratoire de Physique des Solides
Université Paris-Sud
https://www.stem.lps.u-psud.fr/
odile.stephan@u-psud.fr; alexandre.gloter@u-psud.fr

Université Paris Sud – Comprendre le monde, construire l'avenir®
université PARIS-SACLAY
cnrs
metsa
esteem3
Equipement d'excellence TEMPOS – Transmission Electron Microscopy at Palaiseau Orsay Saclay

STEM imaging and EELS

Part I: introduction to Transmission Electron Microscopy / STEM imaging
Part II: spectroscopy at the atomic scale/ STEM EELS (Electron Energy-Loss Spectroscopy)

STEM imaging & EELS principles

A few generalities about transmission microscopy

Image formation principles in STEM and examples

EELS principles and examples

Application to oxide thin films. Some examples below:

1) Octahedra rotation in (La,Sr)MnO3/SrTiO3 superlattices

2) Charge control in manganite by ferroelectric switching in

CaMnO3/BiFeO3 based Mott transistor

3) Orbital ordering in LaAlO3/SrTiO3 bilayers

Few perspectives on STEM-EELS for oxides / interfaces studies

Spectromicroscopy in a STEM

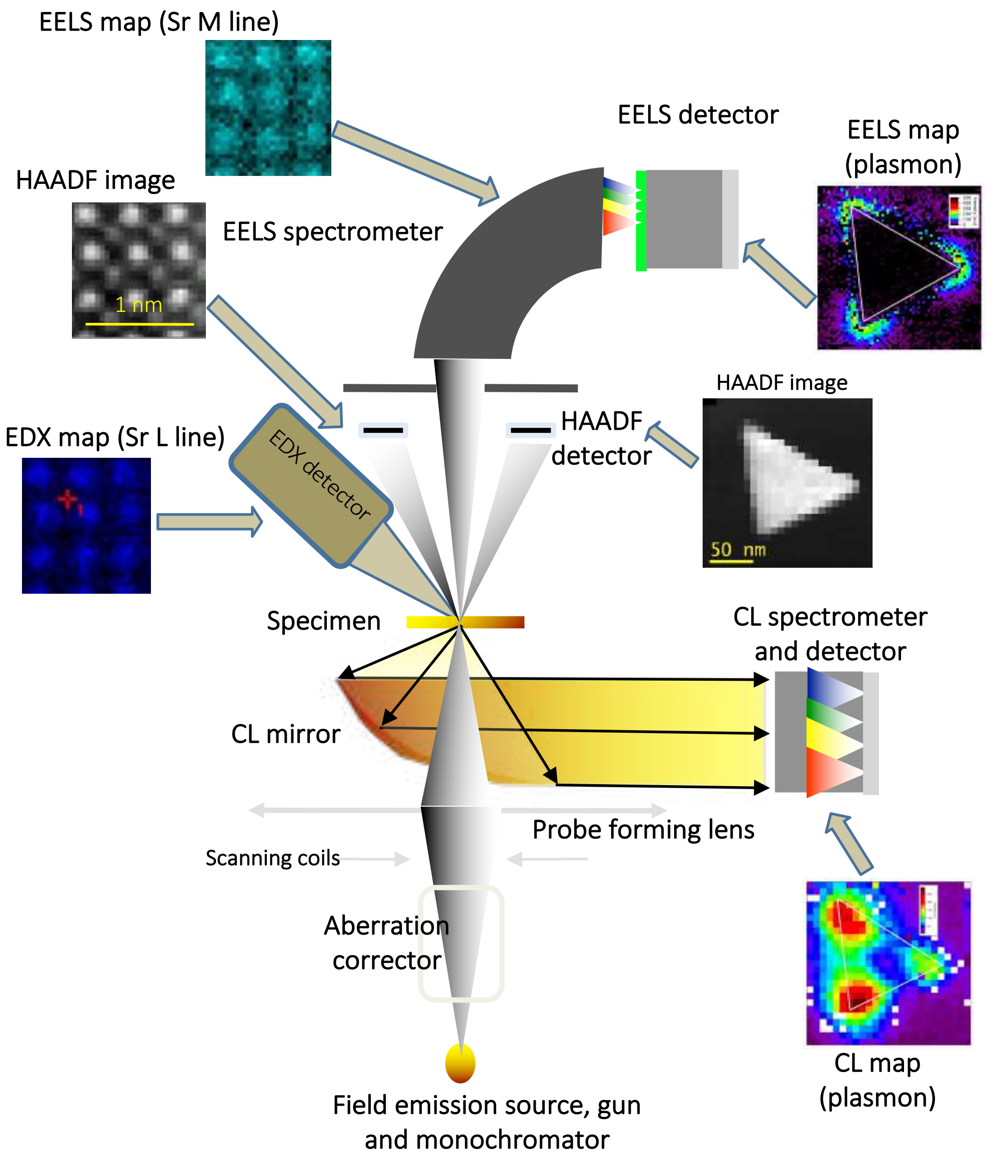

The multisignal approach

EELS spectroscopy : spectral domains

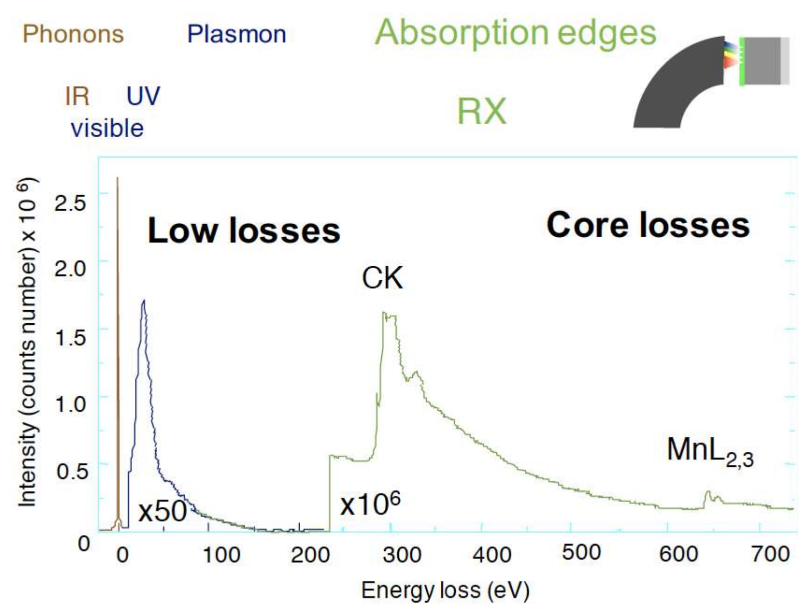

Hyperspectral imaging

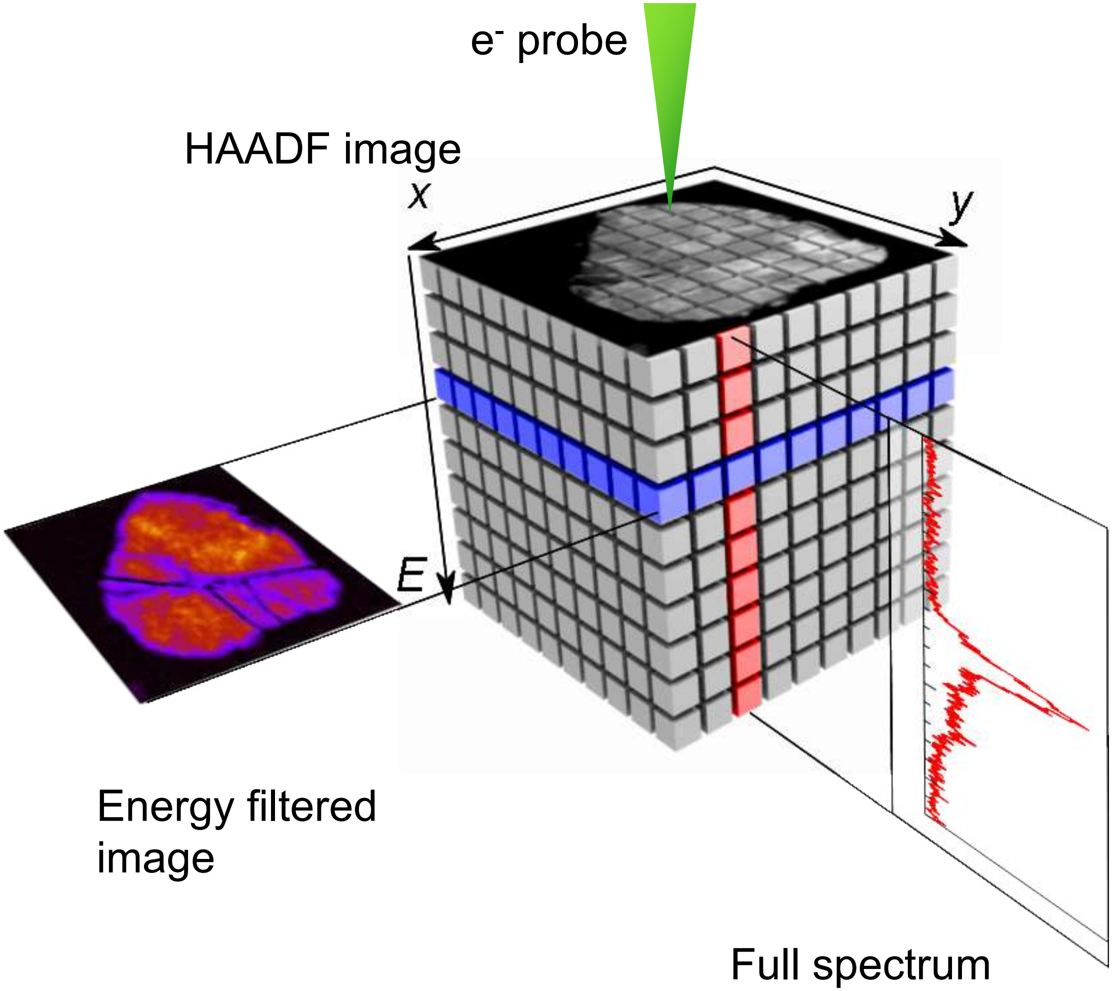

Hyperspectral imaging

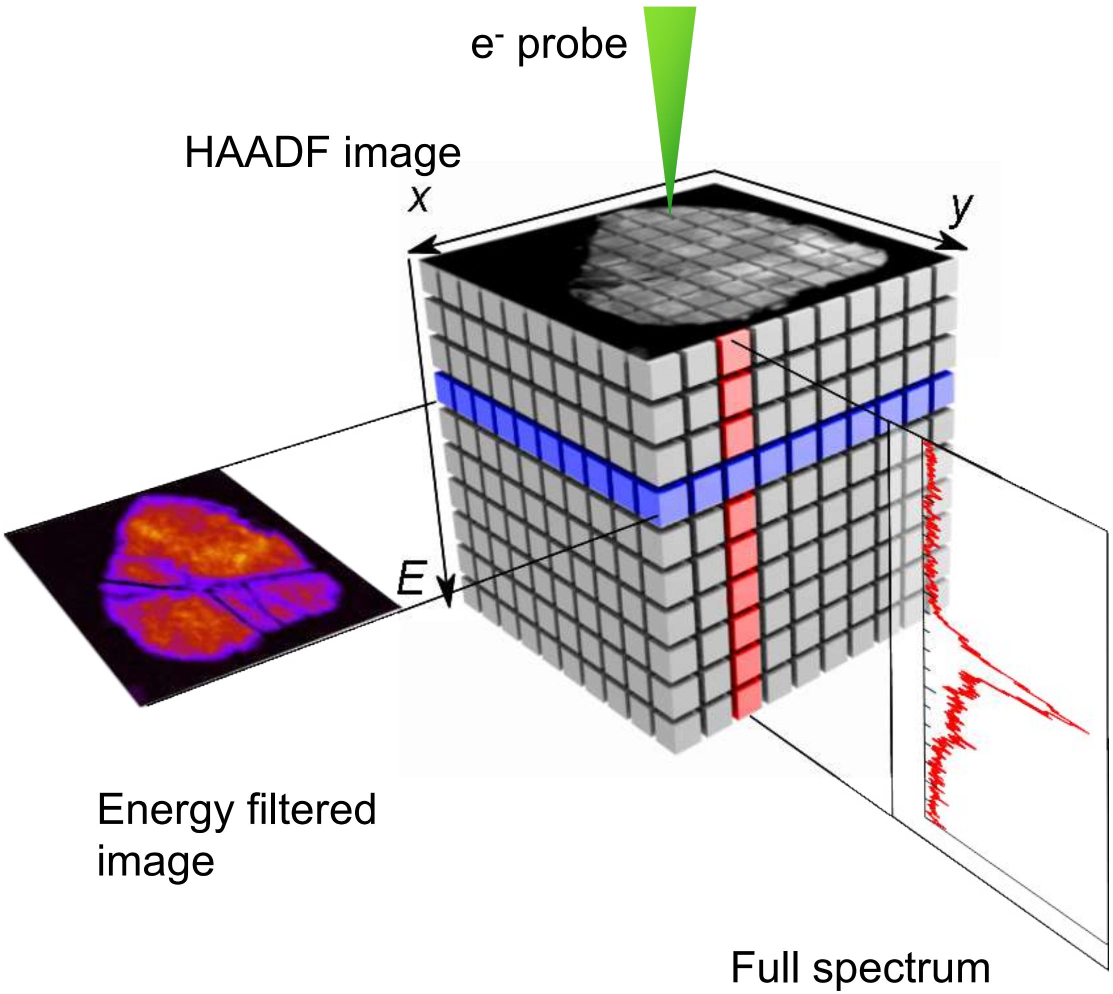

CL spectrum

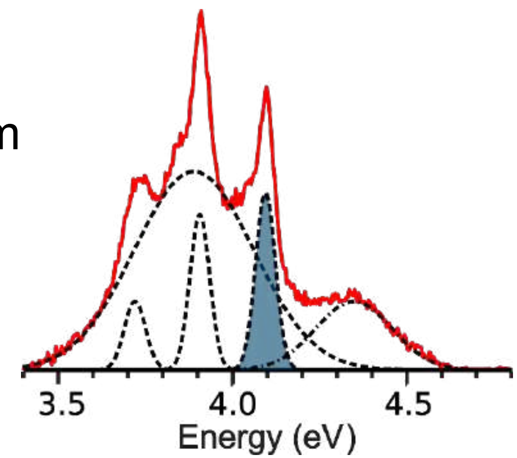

CL Intensity map

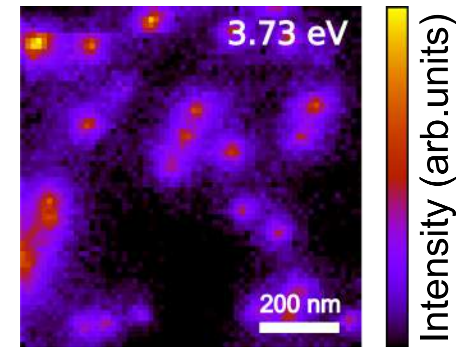

EELS Elemental map

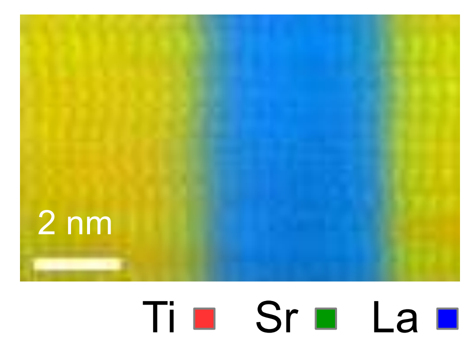

EELS Scattering geometry

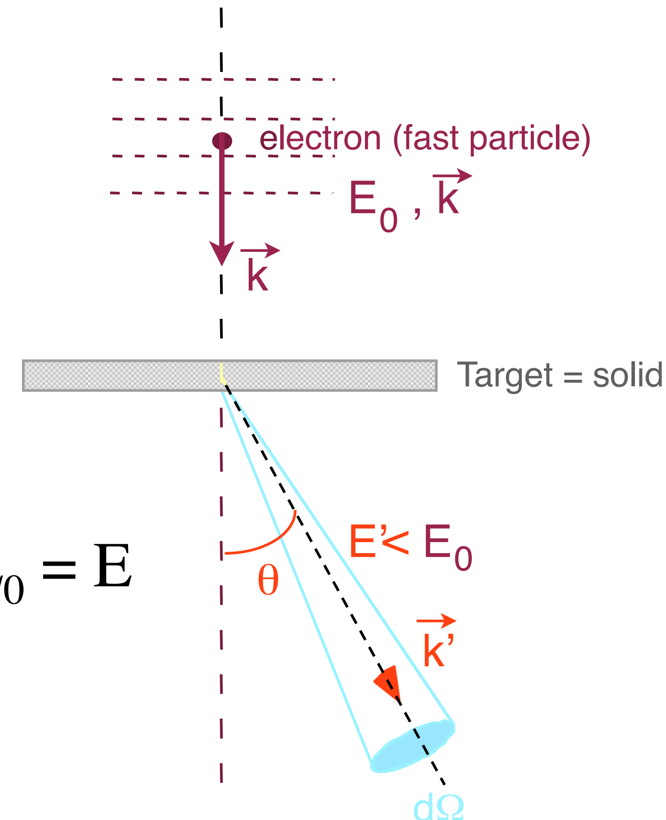

$$E' - E_0 = E$$

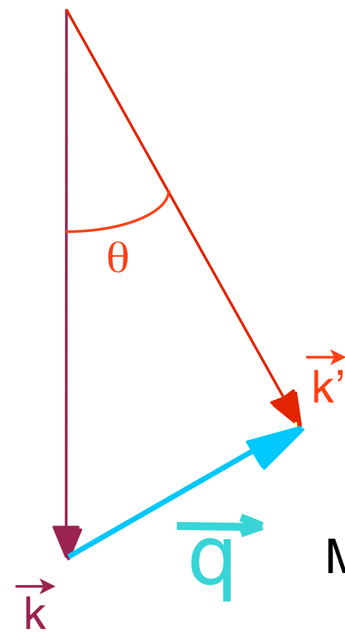

Measured quantities:

$$\frac{d^2 \mathbf{s}(E,q)}{dE\,d\Omega}$$

Momentum transfer $\vec{q}$

Energy loss E

How to measure E?

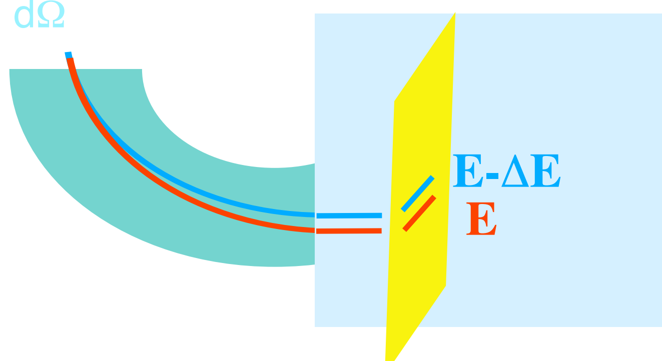

EELS: involved electron populations and associated transitions

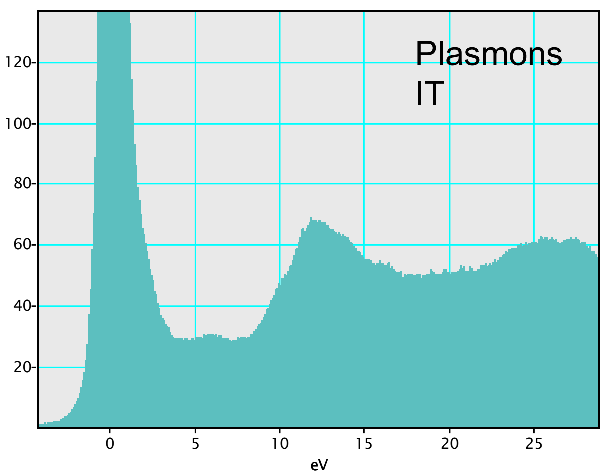

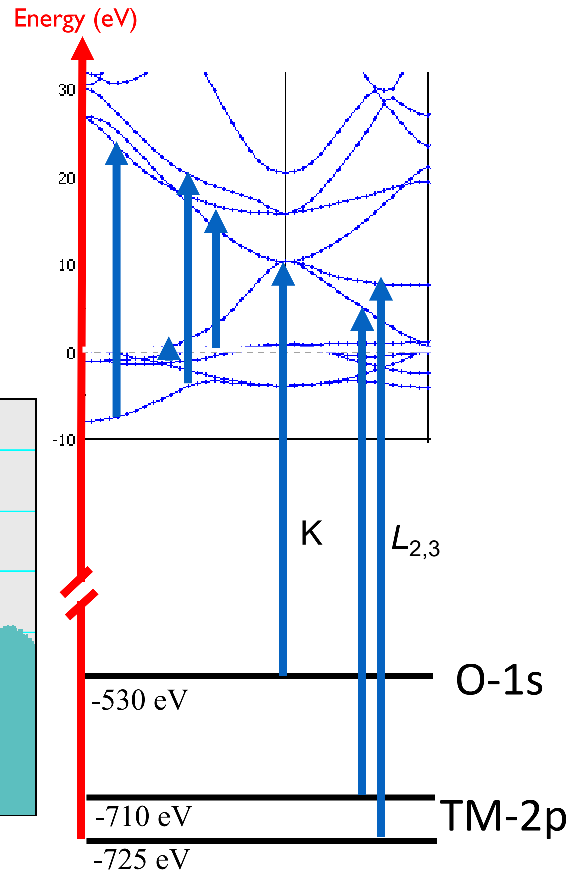

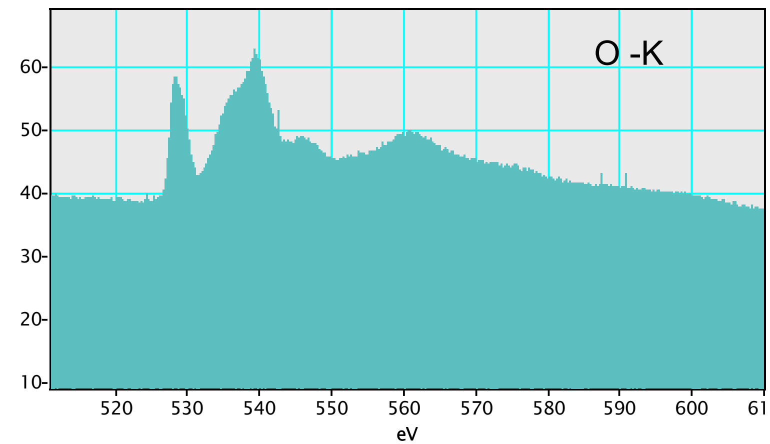

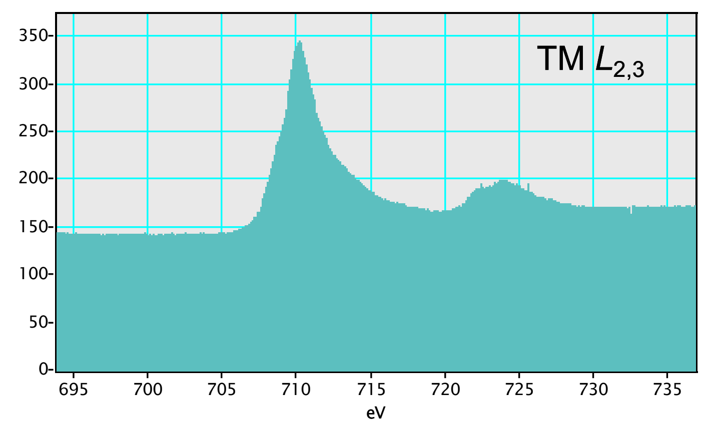

EELS gives informations on the elemental composition of a material (down to the atomic scale)

EELS gives informations on the electronic structure but it is usualy not a direct probe of the Ground State

Comparison between the XAS and EEELS x-sections

$$\sigma(\hbar\omega) = 4\pi^2 \varepsilon\hbar\omega \sum_F \left| \left\langle \Psi_F \left| \sum_i \vec{\varepsilon}.\vec{r}_i \right| \Psi_I \right\rangle \right|^2 \delta(E_i - E_f - \hbar\omega)$$

where **e** is the polarisation vector of the electromagnetic field

$$\frac{\partial^2\sigma}{\partial E \partial\Omega} = \frac{4\gamma^2}{a_0^2 q^4} \frac{k_f}{k_i} \sum_F \left| \left\langle \Psi_F \left| \sum_i \vec{q}.\vec{r}_i \right| \Psi_I \right\rangle \right|^2 \delta(E_i - E_f - E)$$

Where $\mathbf{q} = \mathbf{k}_f - \mathbf{k}_i$ is the transferred momentum called the diffusion vector or the scattering vector

→ **q** and **ε** may play a similar role

In case of an uniaxial symmetry

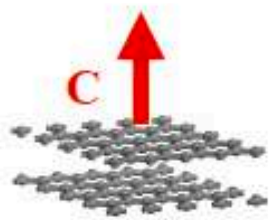

If **q** or ε are // to the z axis, only Δm = 0 that means for a transition from a 1s core state, only the transition to a p_z state are allowed. 1s → π*

If **q** or ε are within the x,y plane, Δm = +1,-1 then transition to state with σ* hybridization are allowed for graphite . 1s → σ*

I(Δm = 0)-I(Δm = +1,-1) is usually called the Linear Dichroic signal

Caution: just like in XAS, for TM, this picture is not truly valid
There is a trade of between momentum and spatial resolution

Absorption edges accessible with EELS

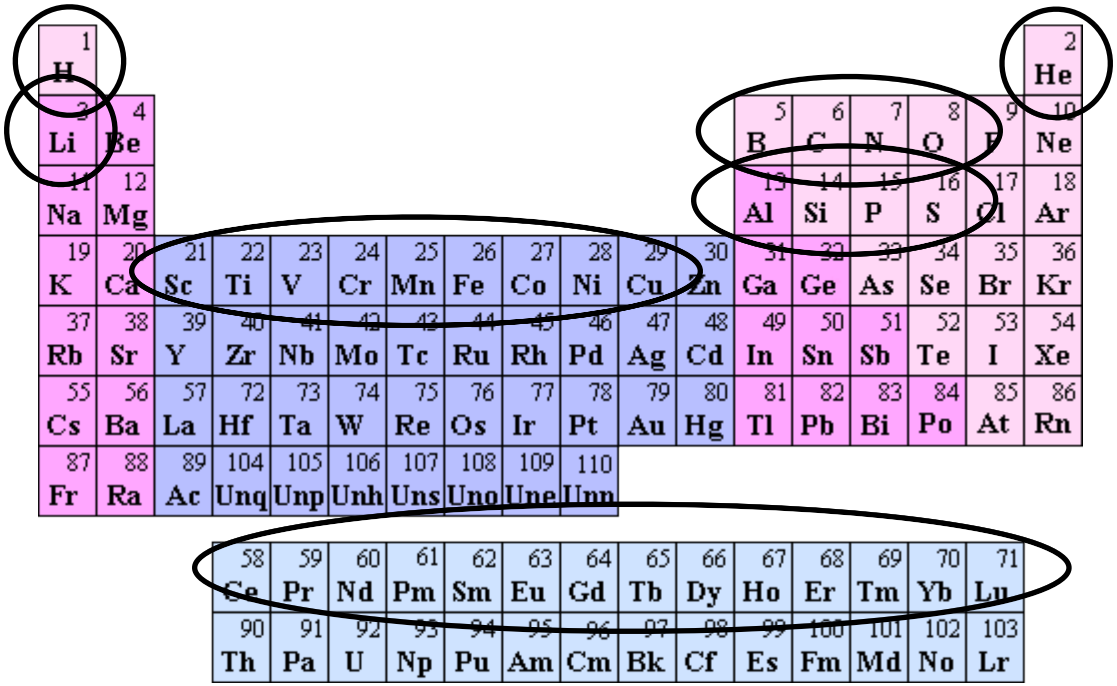

H 1s	13 eV
He 1s	24 eV
Li 1s	55 eV
B,C,N,O 1s	180 eV - - 530 eV
Mg, Al, Si 1s	1300 eV - - 1900 eV
P, S, Cl 1s	2100 eV - - 2900 eV
Mg, Al, Si 2p	50 eV - - 100 eV
P, S, Cl 2p	130 eV - - 200 eV
TM 1s	3900 eV - - 9000 eV
TM 2p	350 eV - - 900 eV
TM 3p	40 eV - - 80 eV

- X-section , - Probe intensity, - Damage…

EELS domain is usually limited from 1 to 2000 eV….

EELS characteristic core-level signals in STO/LAO

Log scale

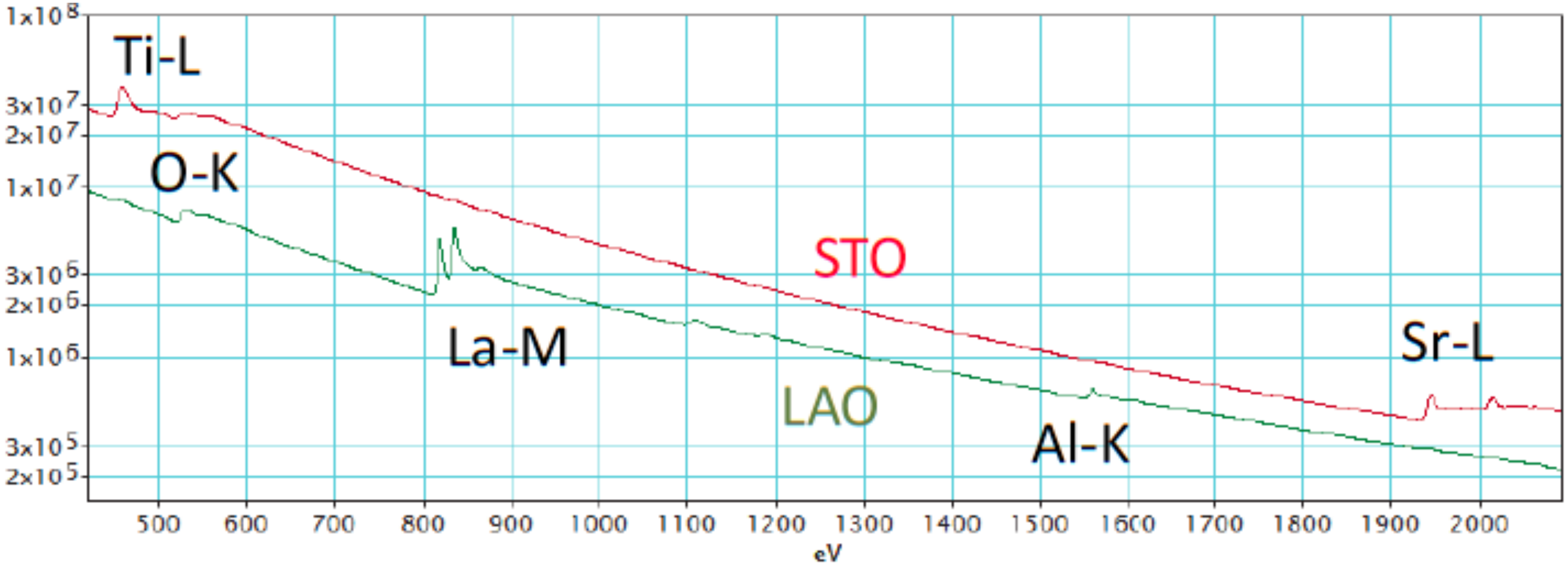

Courtesy G. Tieri & A. Gloter (CNRS-Orsay-France); sample JM. Triscone (U. Geneva).

Large intensity dynamics and spectral range

Core-loss EELS
Elemental analysis of PTO/STO superlattices

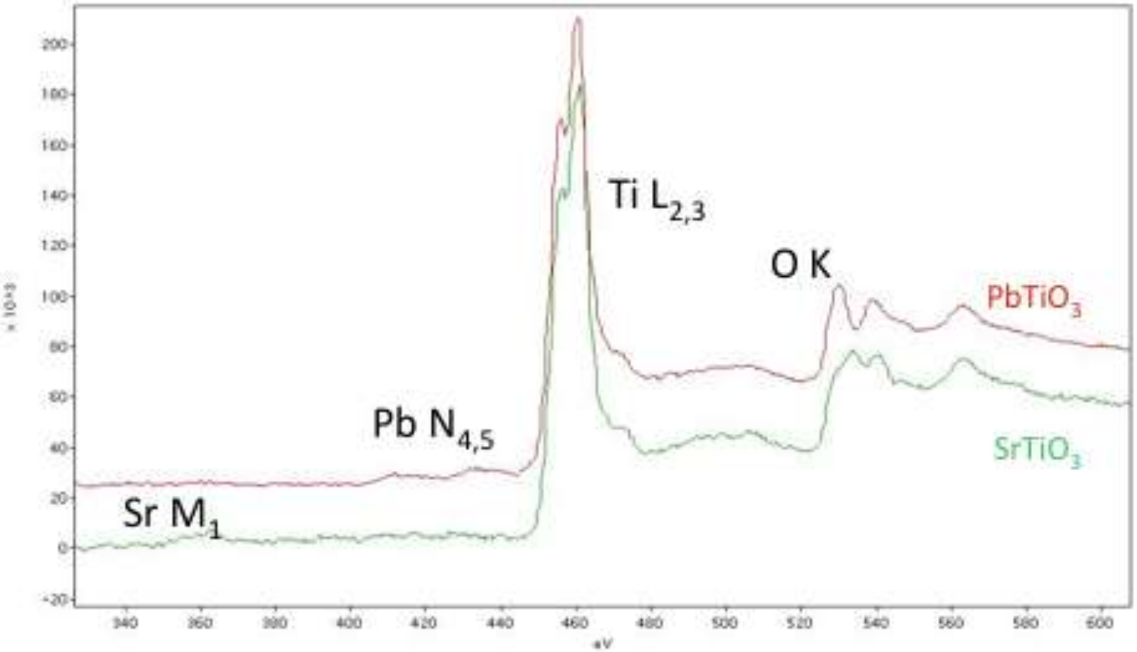

Mapping the intensity of the characteristic edges

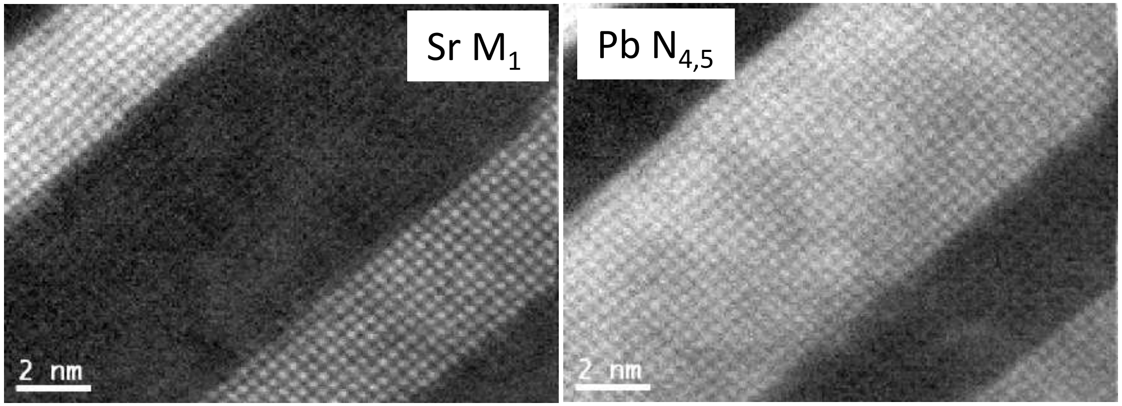

Negligible Sr-Pb interdiffusion in $SrTiO_3$-$PbTiO_3$ superlattices as evidenced by the EELS Sr M_1 (346-370 eV) and Pb $N_{4,5}$ (403-440 eV) signals.

STEM-HAADF, pixels size 9pm, 200 keV, 60pA, spots at 0.86 angstrom are seen in FFT.
STEM-EELS, pixel size 64pm, 5 ms per spectrum, 625 meV/ch, 200 keV, 60pA.

Courtesy K. March, A. Gloter, M. Kociak, M. Tence, A. Torres-Pardo (CNRS-Orsay-France); sample JM. Triscone (U. Geneva).

EELS at the core-loss is sensitive to TM charge (now not so far from XAS)

Fe $L_{2,3}$ edges
$2p^6 3d^n \rightarrow 2p^5 3d^{n+1}$

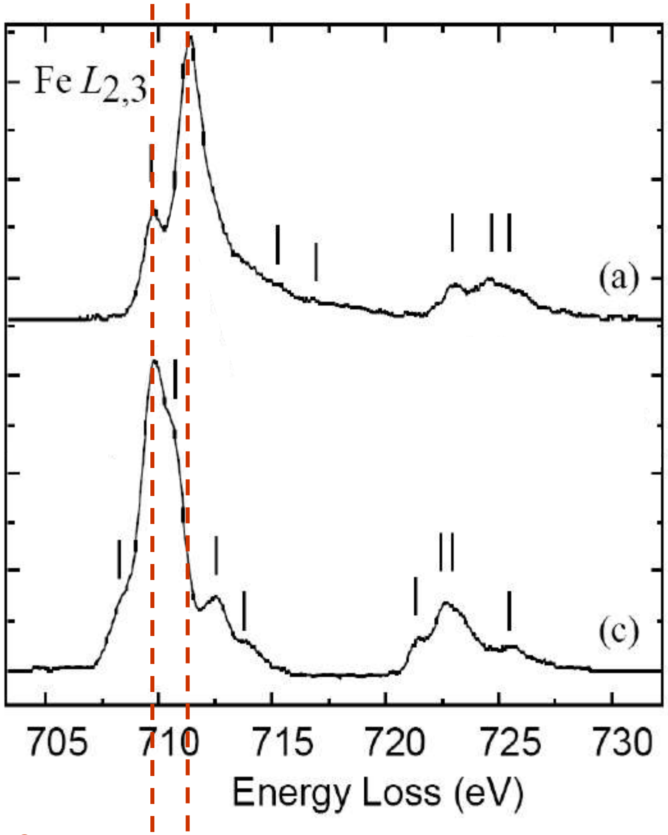

Fe^{3+} (d^5)
Fe_2O_3 hematite

Fe^{2+} (d^6)
$FeCO_3$ siderite

Gloter et al.,Ultramicroscopy 96, 385, (2003)

Ferrous-ferric iron
Chemical shift of L3 line maximum of 1.6 - 2 eV

TM 2p edges ($TiL_{2,3}$) : Origin of the peaks

Classic scheme for 3d orbitals crystal field splitting and 2p / $L_{2,3}$ excitation

TiO_2

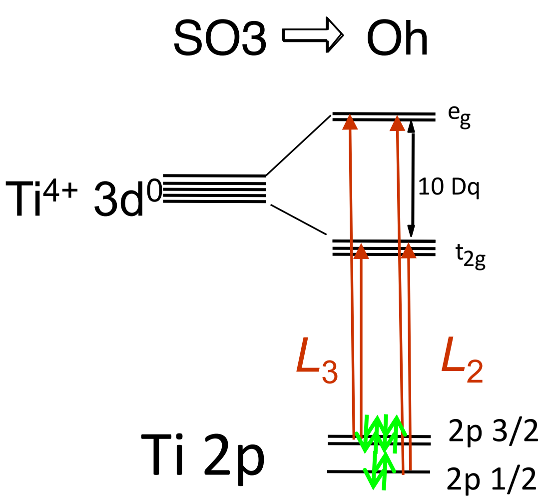

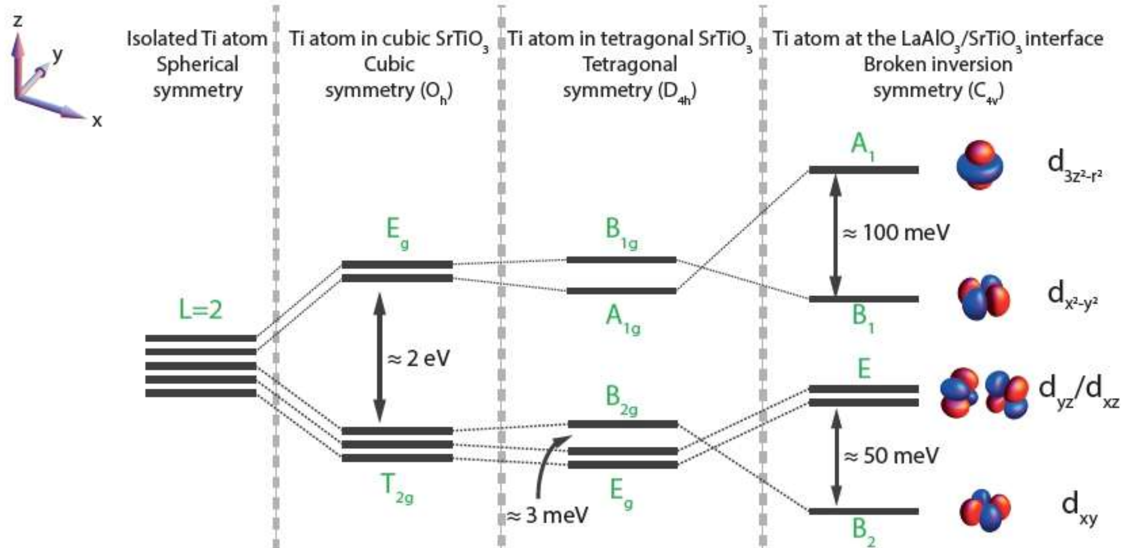

Figure 2.5: Energy of the Ti 3*d* orbitals in the presence of crystal field. Energy levels of the Ti 3*d* orbitals in a spherical, cubic, tetragonal and non inversion-symmetric tetragonal environment. The splittings were determined from experimental and theoretical studies [50–55]. The green labels refer to the irreducible representation to which the orbital(s) belong(s).

EELS principles: fine structures mapping

Measuring the crystal, field splitting across a $SrTiO_3$-$PbTiO_3$ interface by the EELS Ti $L_{2,3}$ edges fine structures evolution.

206x161 spim images, 50pm pixel size, 10 ms per spectrum, 90 meV/ch, 200 keV, 60pA, raw EELS data. Courtesy A. Gloter, M. Kociak, M. Tence, A. Torres-Pardo (CNRS-Orsay-France), sample JM. Triscone (U. Geneva).

A.Torres-Pardo et al., Phys. Rev. B 84, 220102 (2011).

P. Zubko et al. Nano Letters 12(6), 2846 (2012).

Coll. J.M. Triscone
U. Geneva

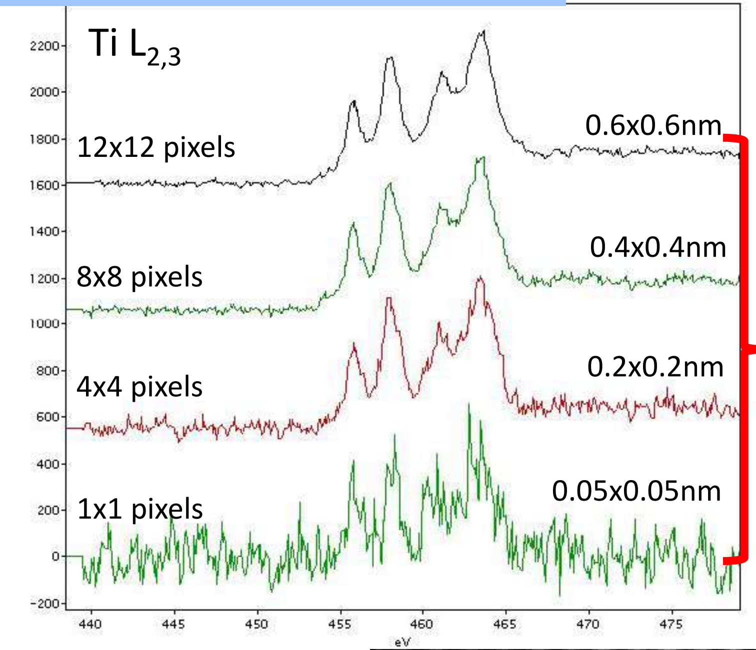

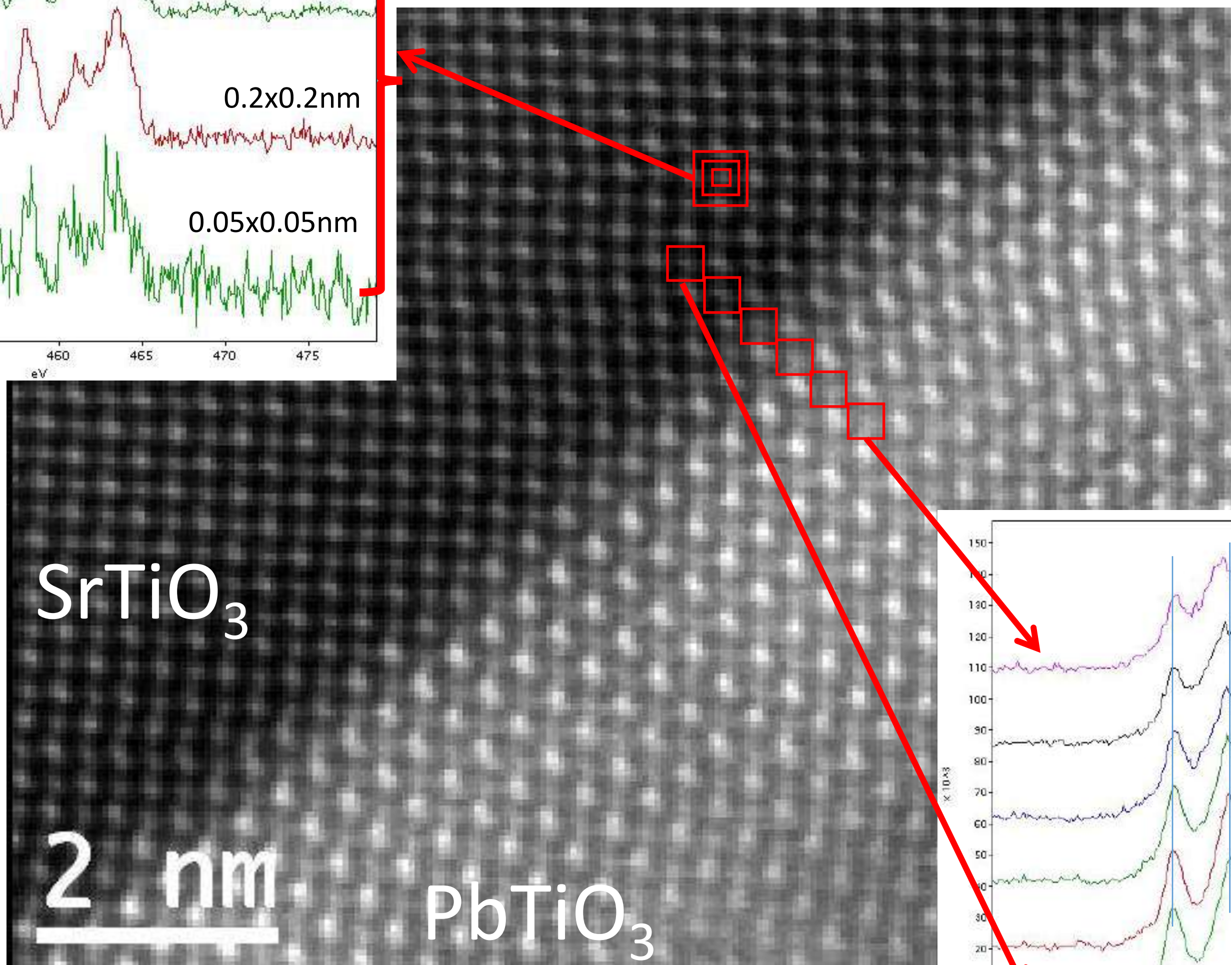

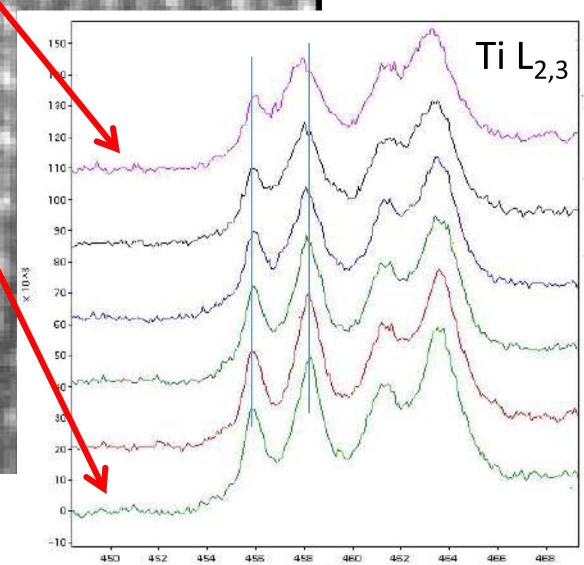

Spectromicroscopy up to 100.000 spectra
Unit cell resolved fine structures on Ti $L_{2,3}$ edges

Thin film : unusual (magnetic) properties

Take one magnetic
One non-magnetic

$(La,Sr)MnO_3$
(Ferro-magnet)

$SrTiO_3$ (non magnetic)

Make heterostructures

$(La,Sr)MnO_3$
(10uc)

$SrTiO_3$
substrate

Still ferro-magnetic

Make smaller heterostructures

$(La,Sr)MnO_3$(4uc)

$SrTiO_3$ (7uc)

$(La,Sr)MnO_3$(4uc)

$SrTiO_3$ (7uc)

$(La,Sr)MnO_3$(4uc)

$SrTiO_3$ (7uc)

$(La,Sr)MnO_3$(4uc)

$SrTiO_3$ substrate

Non magnetic

Interfacial Control of Magnetic Properties at $LaMnO_3/LaNiO_3$ Interfaces

M. Gibert,[*,†] M. Viret,[†,‡] A. Torres-Pardo,[§] C. Piamonteze,[∥] P. Zubko,[†] N. Jaouen,[⊥] J.-M. Tonnerre,[#] A. Mougin,[§] J. Fowlie,[†] S. Catalano,[†] A. Gloter,[§] O. Stéphan,[§] and J.-M. Triscone[†]

Nano letters 15, 7355–7361 (2015)

$LaMnO_3$ is Mn^{3+} , Mott insulator with A-type antiferromagnetism in bulk form, becomes ferromagnetic in thin film grown on STO.
$LaNiO_3$ is Ni^{3+}, paramagnetic metal in bulk form, could become insulating and/or AFM in thin films.

Magnetization versus temperature of $(7u.c.LNO/7u.c.LMO)_1$//(001)STO (red), $(7u.c.LMO/7u.c.LNO)_1$//(001)STO (blue) and 7u.c.LNO//(001)STO (grey). A 28u.c. LMO film//(001)STO (black) is also shown.

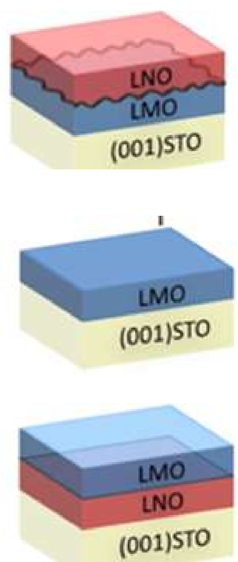

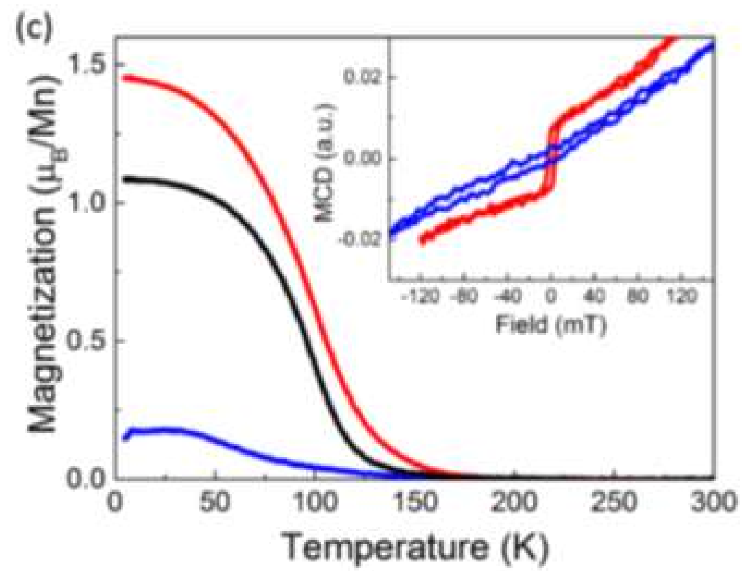

LMO FM is decreased or enhanced in the bi-layers

Structure of the LNO/LMO interfaces in superlattices

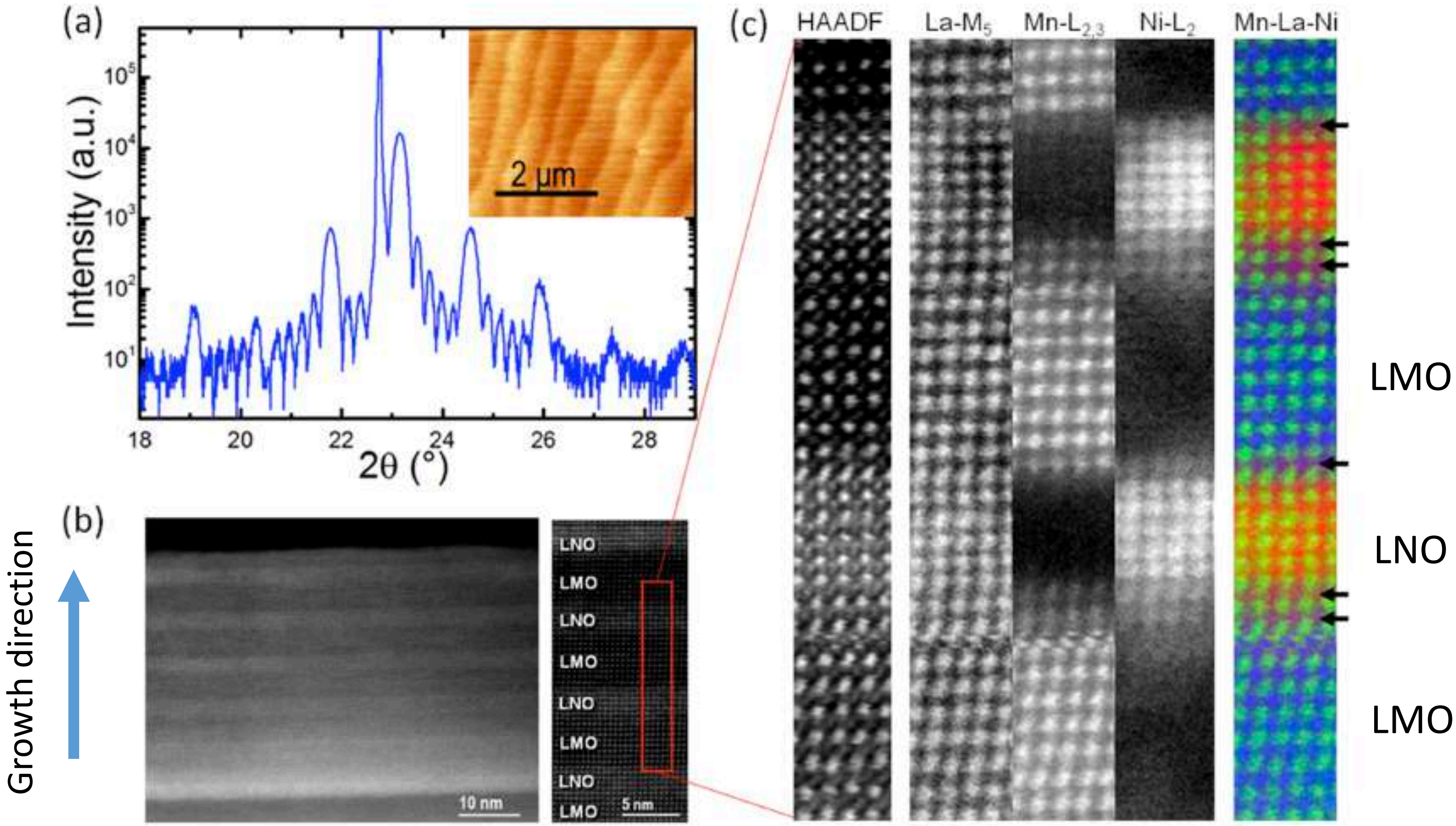

Marta Guibert et al. Nanoletter 2016

(a) XRD scans for a (8LNO/8LMO)6 superlattice grown on (001)STO. Inset: corresponding atomic force microcopy image. (b) Low magnification TEM image. (c) EELS measurements showing the interfacial structural asymmetry (indicated by arrows).

LMO/LNO interface is rougher compared to the LNO/LMO interface

EELS Mn $L_{2,3}$ at the LNO/LMO interfaces

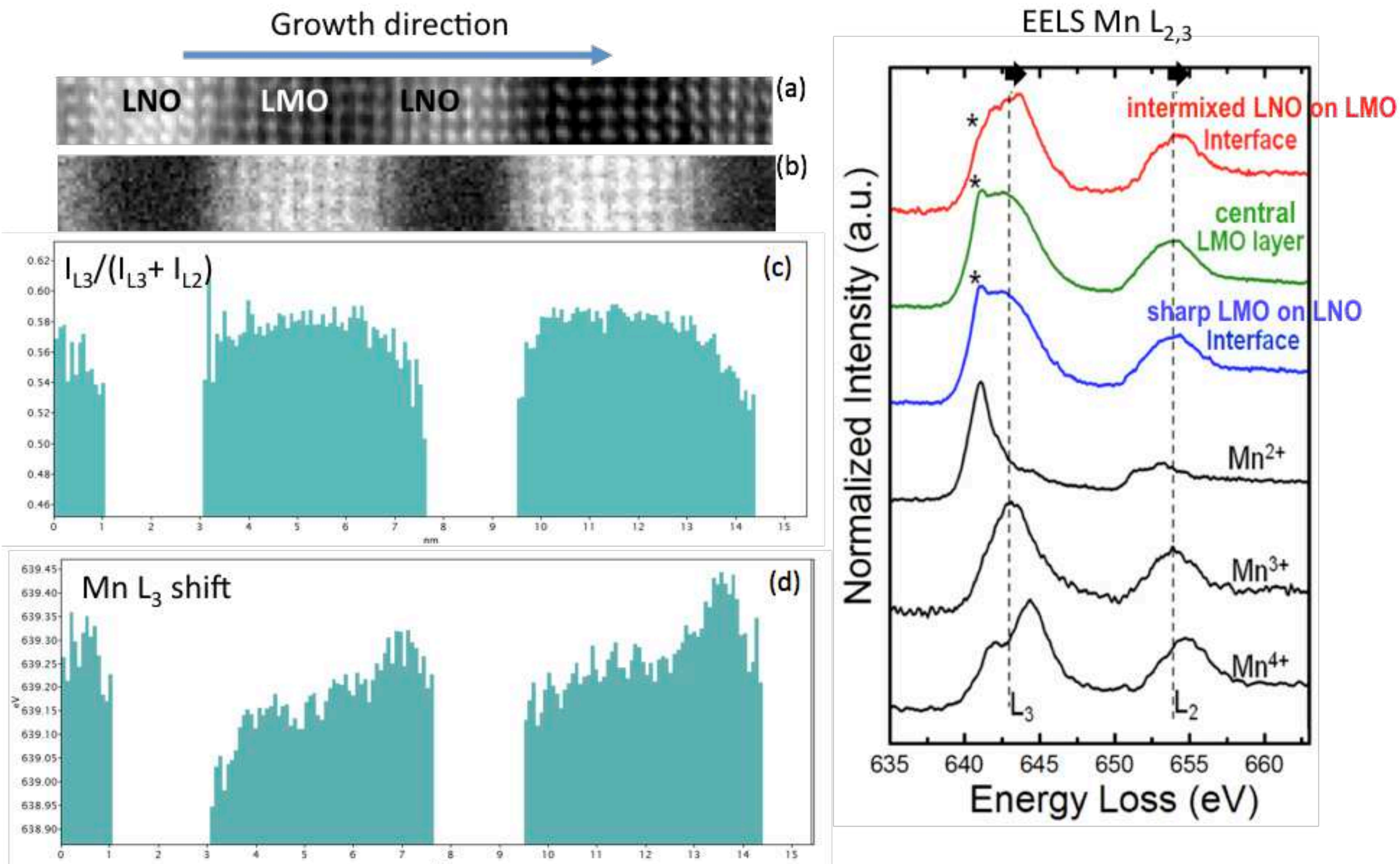

Both energy shifts and branching ratio indicated introduction of more holes (Mn^{4+}) in the rougher LMO/LNO interface compared to the LNO/LMO interface

XAS Mn $L_{2,3}$ of the STO/LMO , STO/LNO/LMO and STO/LMO/LNO

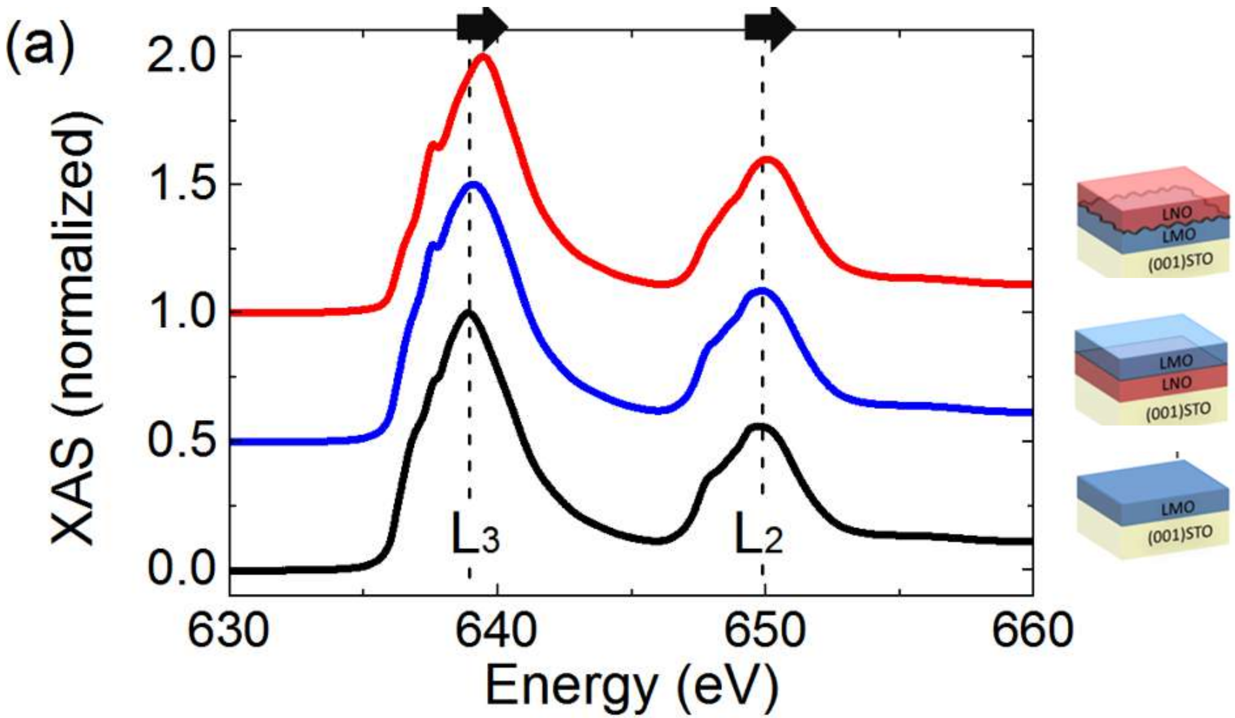

XAS measurements at 2K in 30° grazing incidence in total electron yield (TEY) configuration after field cooling in 0.05T with the field parallel to the sample plan. (C. Piamonetze, PSI, Suisse)

Electron transfer from Mn^{3+}-Ni^{3+} to Ni^{2+}-Mn^{4+} for STO/LMO/LNO

XAS spectral anisotropies (XMCD, XLD)

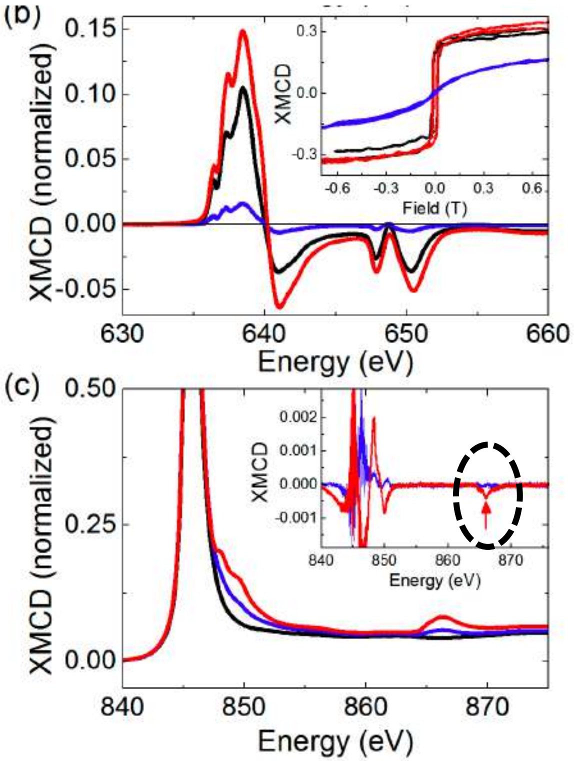

X-ray Magnetic Circular Dichroism (XMCD) shows magnetic Mn (and Ni for the rough interface)

X-ray Linear Dichroism (XLD) is also observed,

- XLD_{300K} at room temperature evidence orbital anisotropies
- (XLD_{2K_1T} - XLD_{300K}) and (XLD_{2K_0T}-XLD_{300K}) provide information about FM and AFM ordering

EELS – XAS – XMCD – XLD indicate that

1) (STO [100])-LMO-LNO is rough with Mn^{4+}-Ni^{2+} charge distribution at the interface.

The Ni^{2+}- Mn^{4+} interact ferromagnetically accordingly to Goodenough-Kanamori rules, like in the case of the insulating ferromagnetic double-perovskite La_2NiMnO_6

2) (STO [100])-LNO-LMO is sharp, with Mn^{3+}-Ni^{3+} charge distribution at the interface.

Presence of a canted-antiferromagnetic order in the LMO layer

M. Gibert et al., Interfacial Control of Magnetic Properties at LaMnO3/LaNiO3 Interfaces, Nano letters 15, 7355–7361 (2015)

Thin film : unusual (magnetic) properties

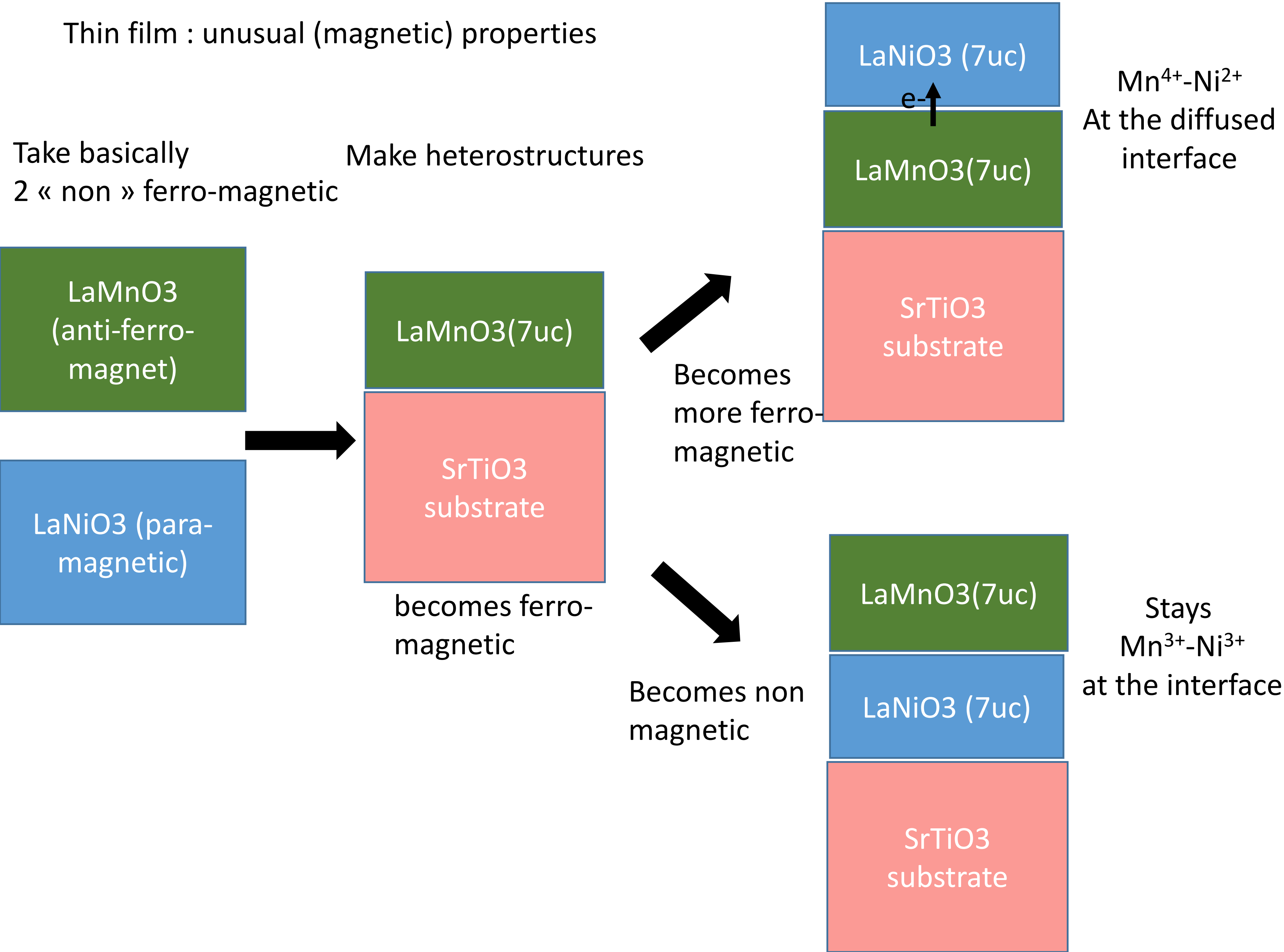

Charge quantification at interfaces, which sensitivity?

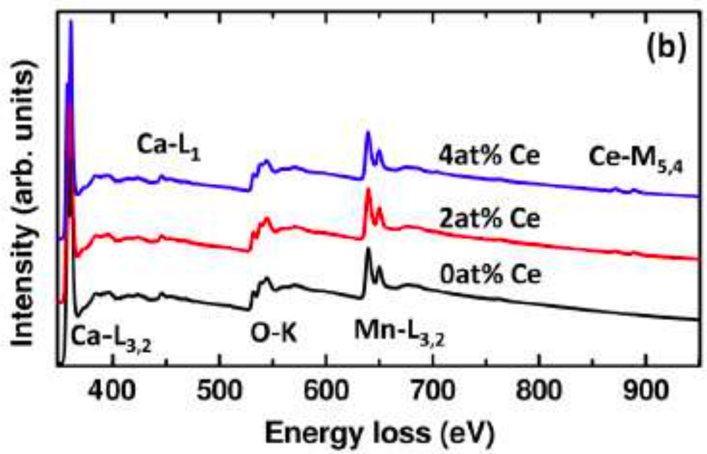

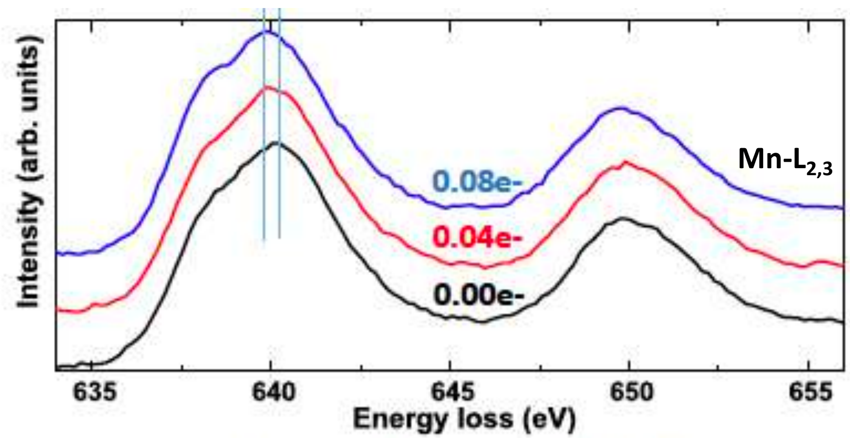

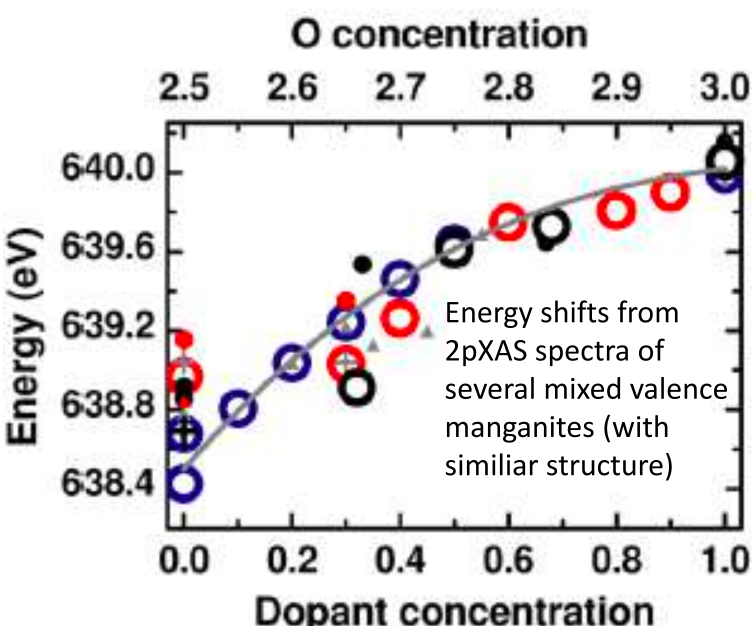

Mn^{3+} Mn^{4+}

Excess charges at the interfaces

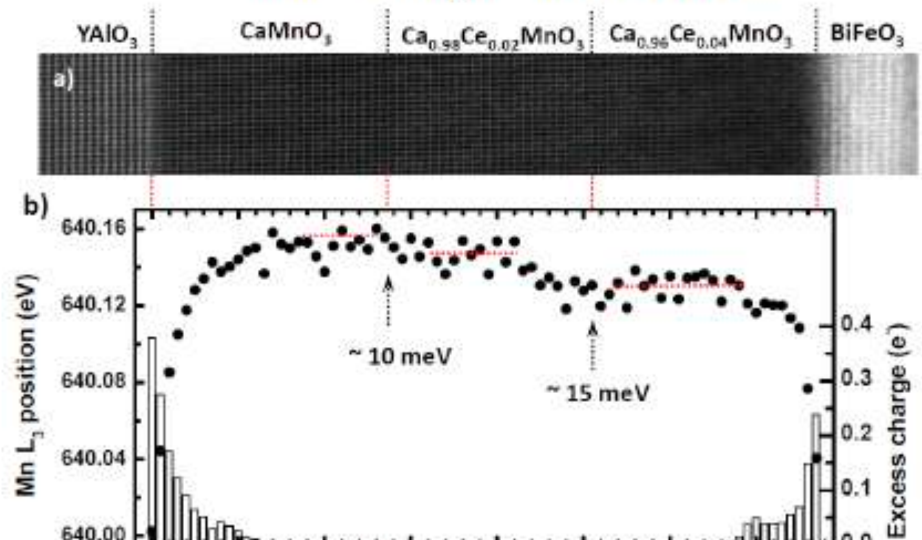

M. Marinova et al. Nanoletters (2015)

Ferroelectric control of a Mott insulator the $Ca_{1-x}Ce_xMnO_3/BiFeO_3$ system

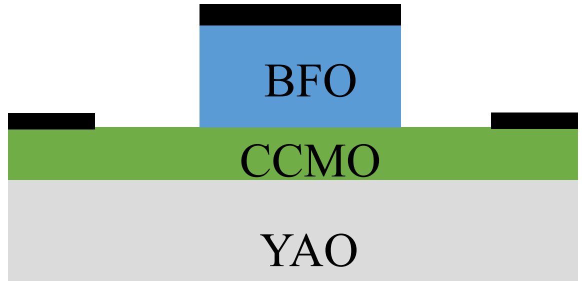

4 nm BFO

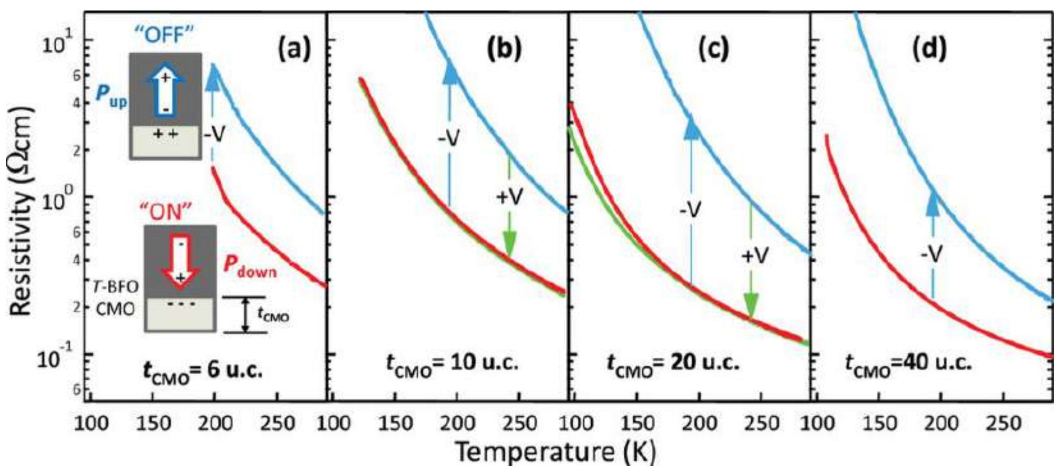

H. Yamada et al. Scientific Reports 3, 2834 (2013).

M. Marinova et al. Nano letters 15 2533 (2015).

30 nm BFO

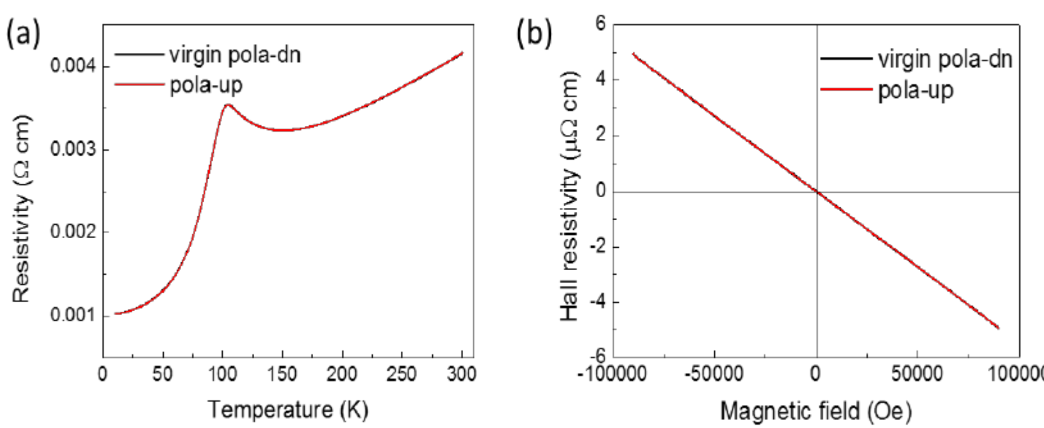

X. Li, in preparation.
No switching between different polarisation states, why?

Coll. V. Garcia et al., UMPhy Thales

EELS examples: measuring charges at interfaces

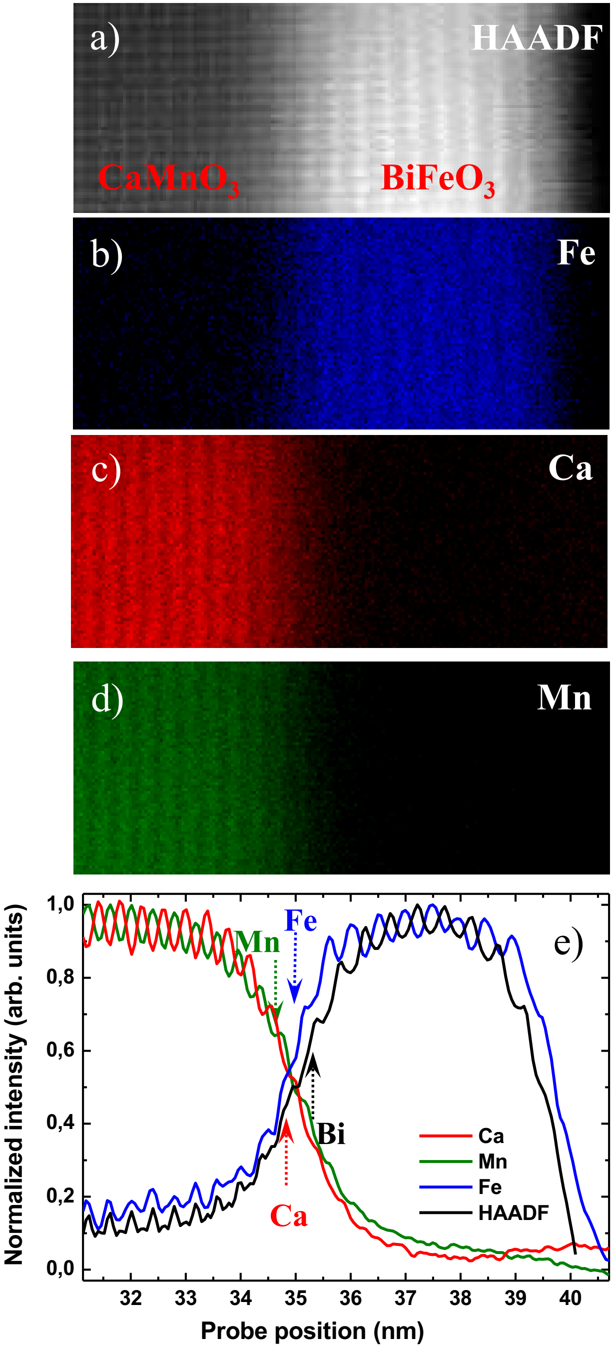

Interface termination planes ($CaMnO_3/BiFeO_3$)

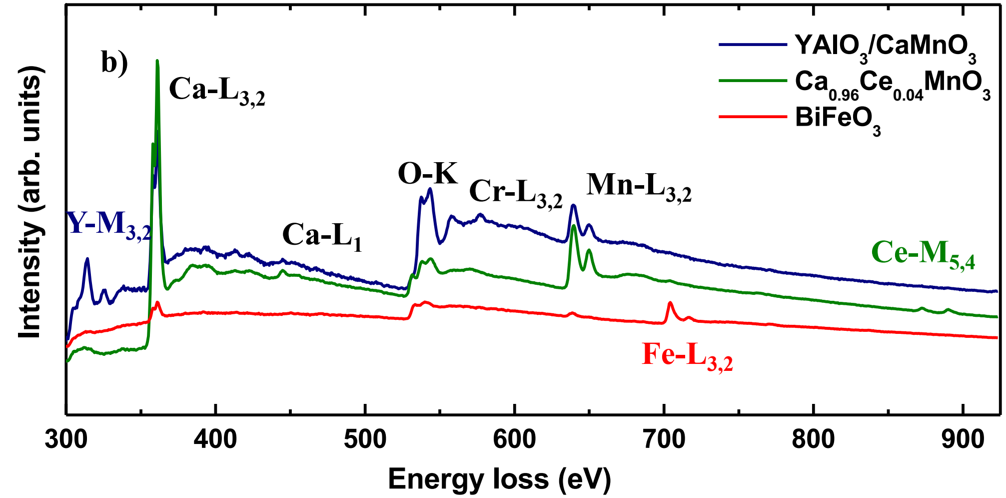

Perovskite ABO_3 : AO plane and BO_2 plane

The observed termination plane sequence is $(CaO)^0$-$(MnO_2)^0$-$(CaO)^0$-$(FeO_2)^{-1}$-$(BiO)^{+1}$-$(FeO_2)^{-1}$

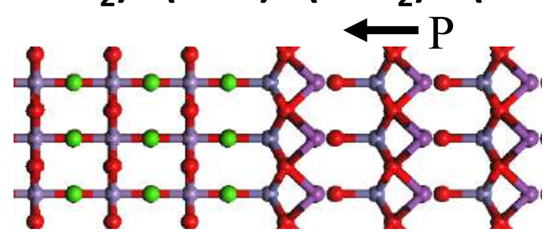

and not $(MnO_2)^0$-$(CaO)^0$-$(MnO_2)^0$- $(BiO)^{+1}$-$(FeO_2)^{-1}$ -$(BiO)^{+1}$

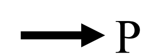

M. Marinova, et al. Nanoletters 2015.

Coll. V. Garcia, S. Fusil, A. Barthélémy, M. Bibes, UMPhy Thales

Ab-initio modeling and role of the interface plane termination

P point towards a…

.....Fe terminated-BFO

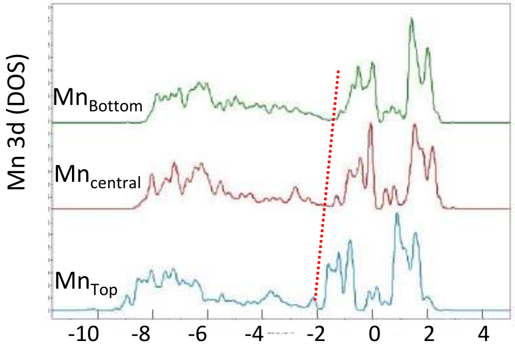

« electron doped »

.....Bi terminated-BFO

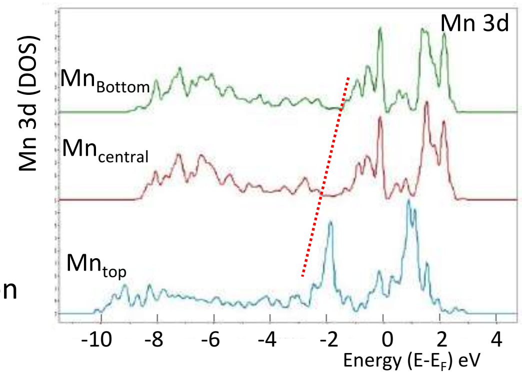

« electron doped »

Polarization pointing toward CMO injects e-

« electron doped »

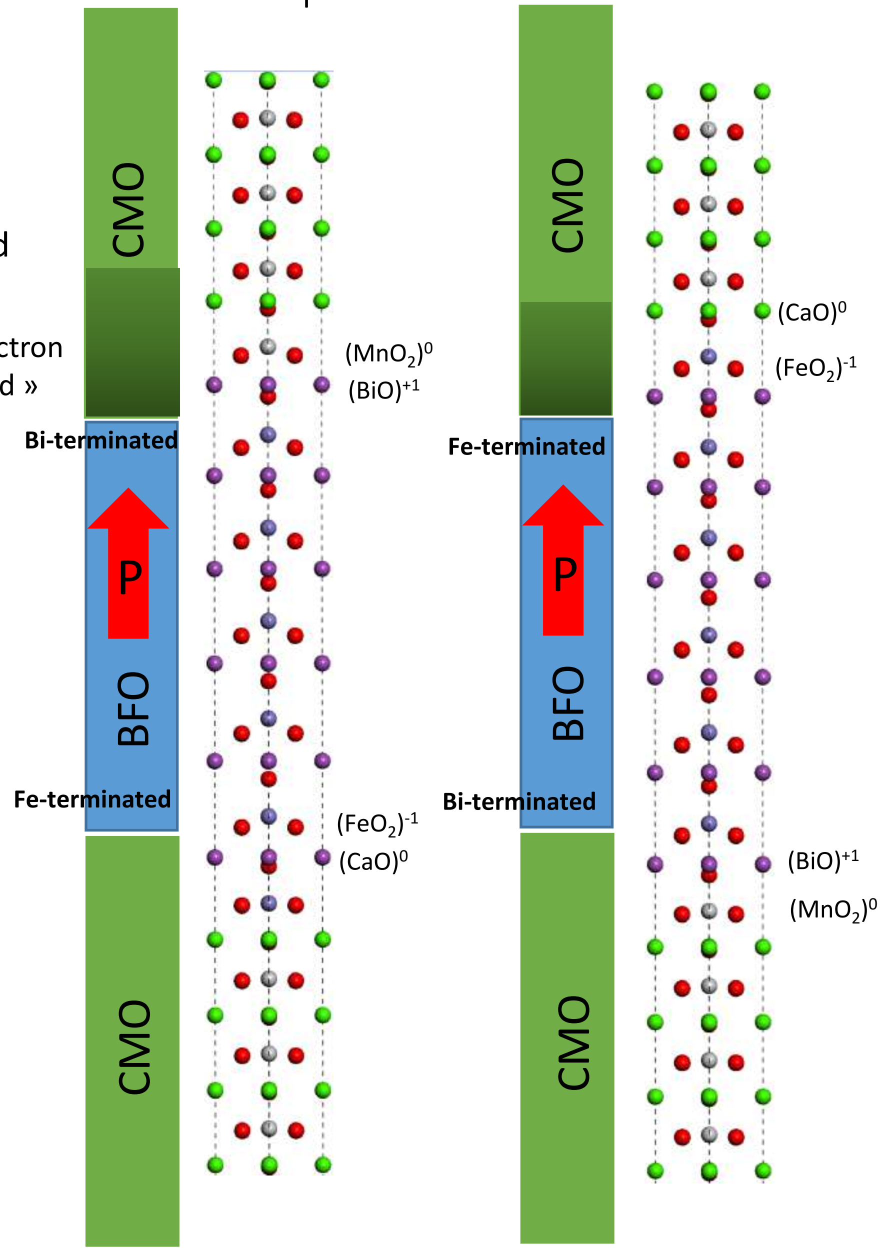

Fe terminated is 1.5 eV lower in total energy

It has less electrons in Mn eg orbitals

It has larger BFO FE structural distortion

Ex-situ polling by electrode or piezo-force microscope + FIB sample preparation

PFM image

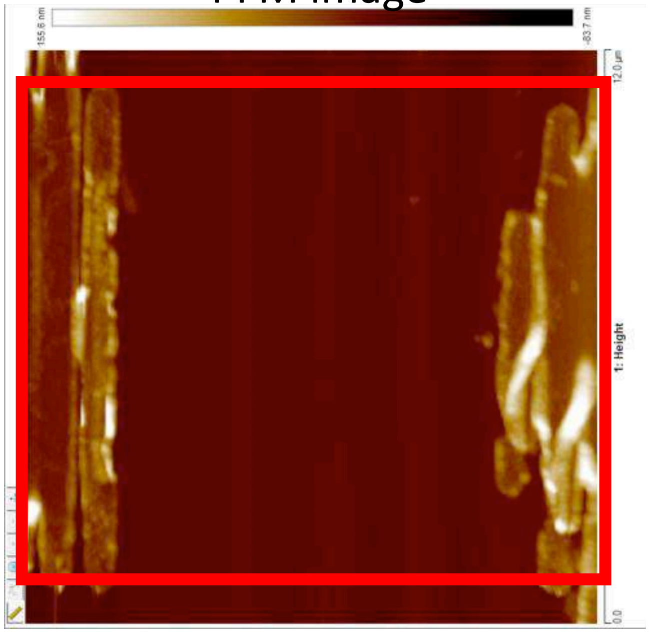

PFM phase image

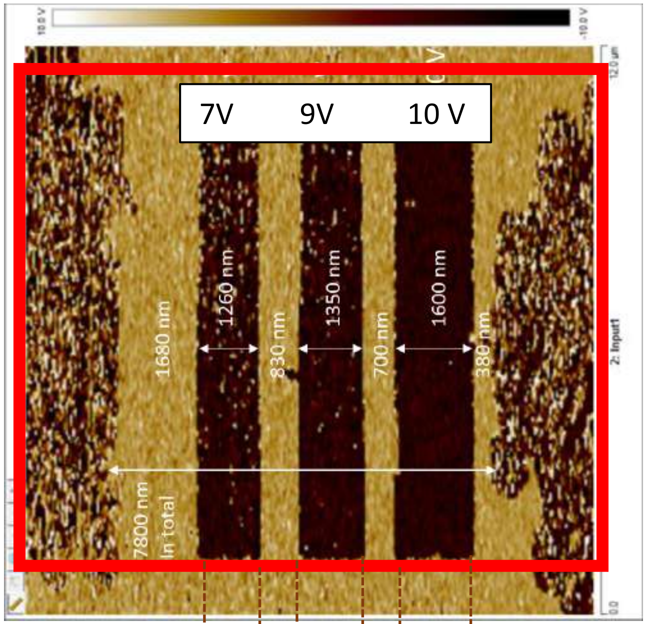

Apparent electrical switching in PFM

SEM image

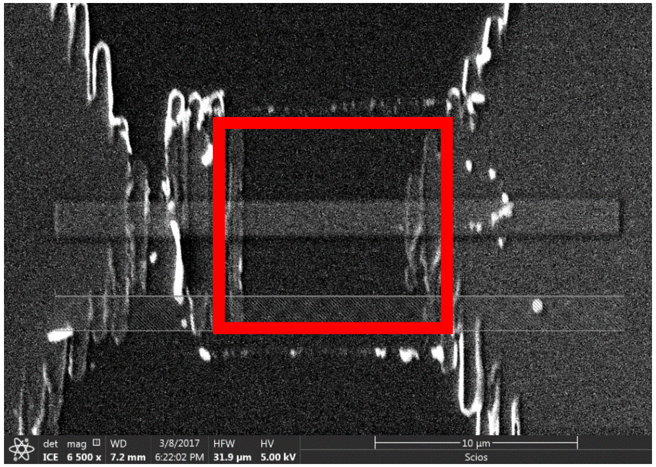

STEM image

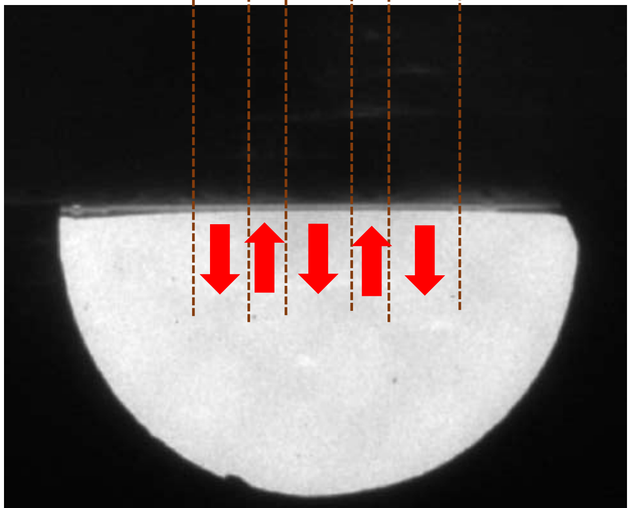

Observation of polarization in $BiFeO_3$ combining ABF and HAADF imaging

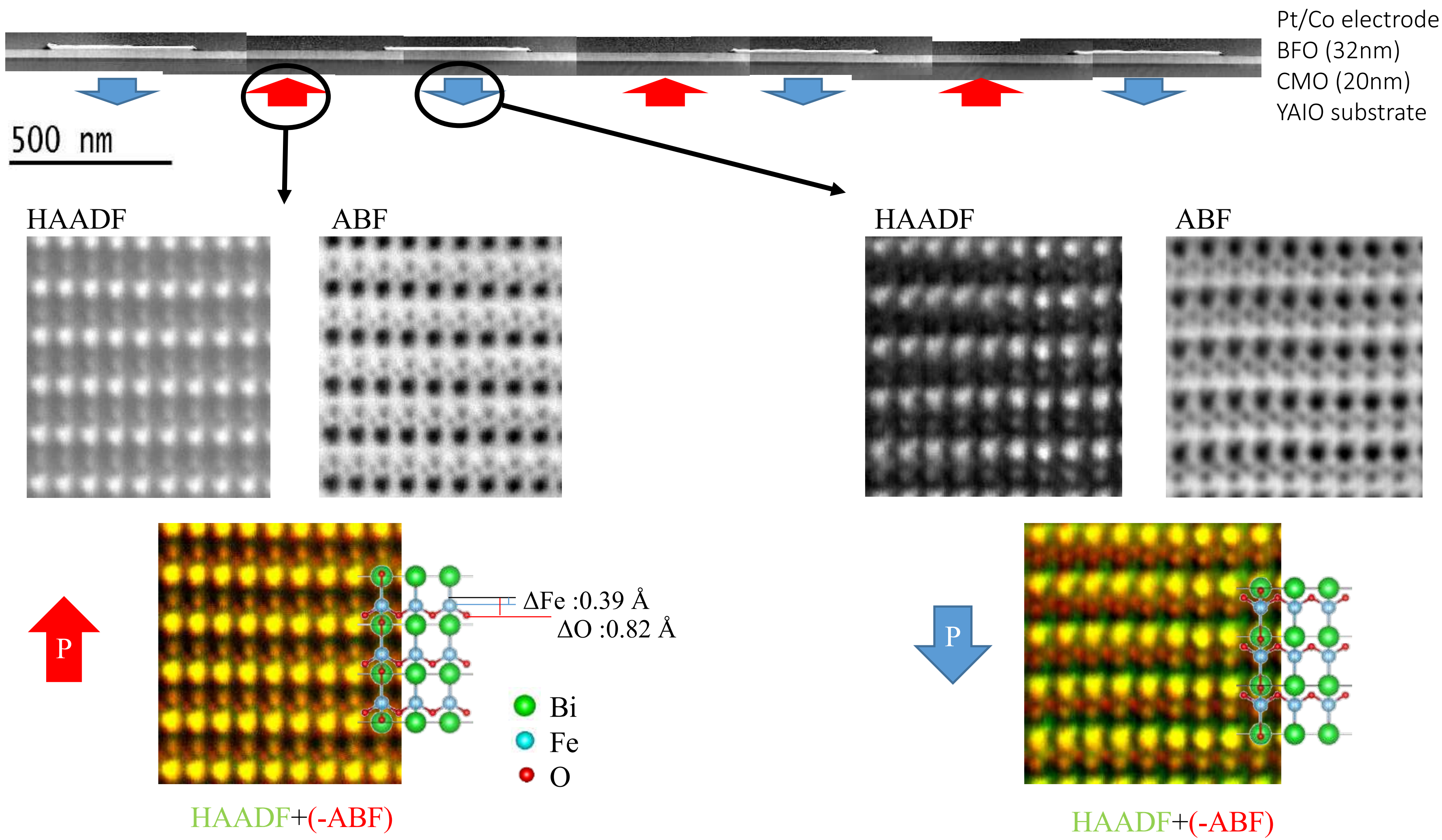

BFO domains

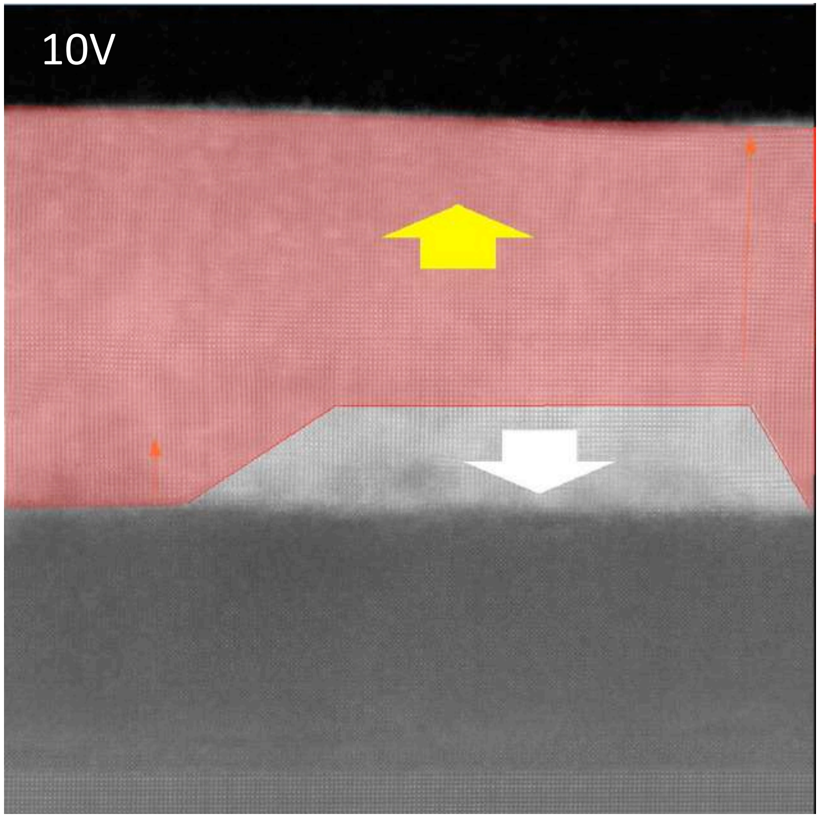

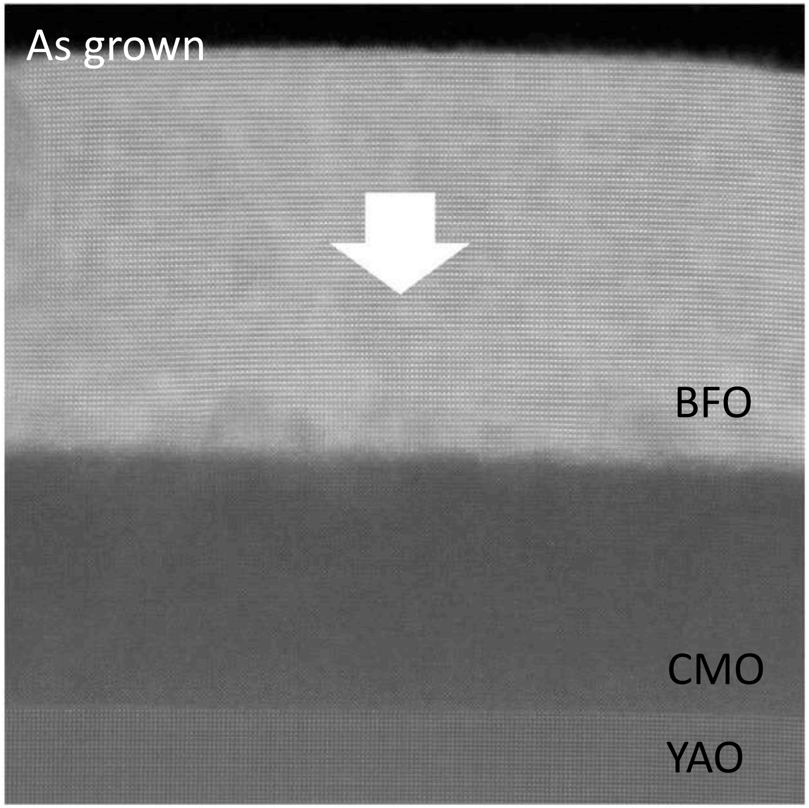

Trends with increasing positive bias

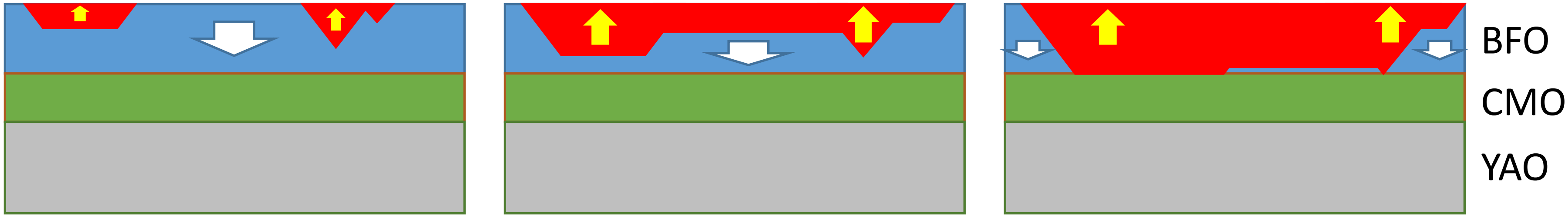

BFO domains

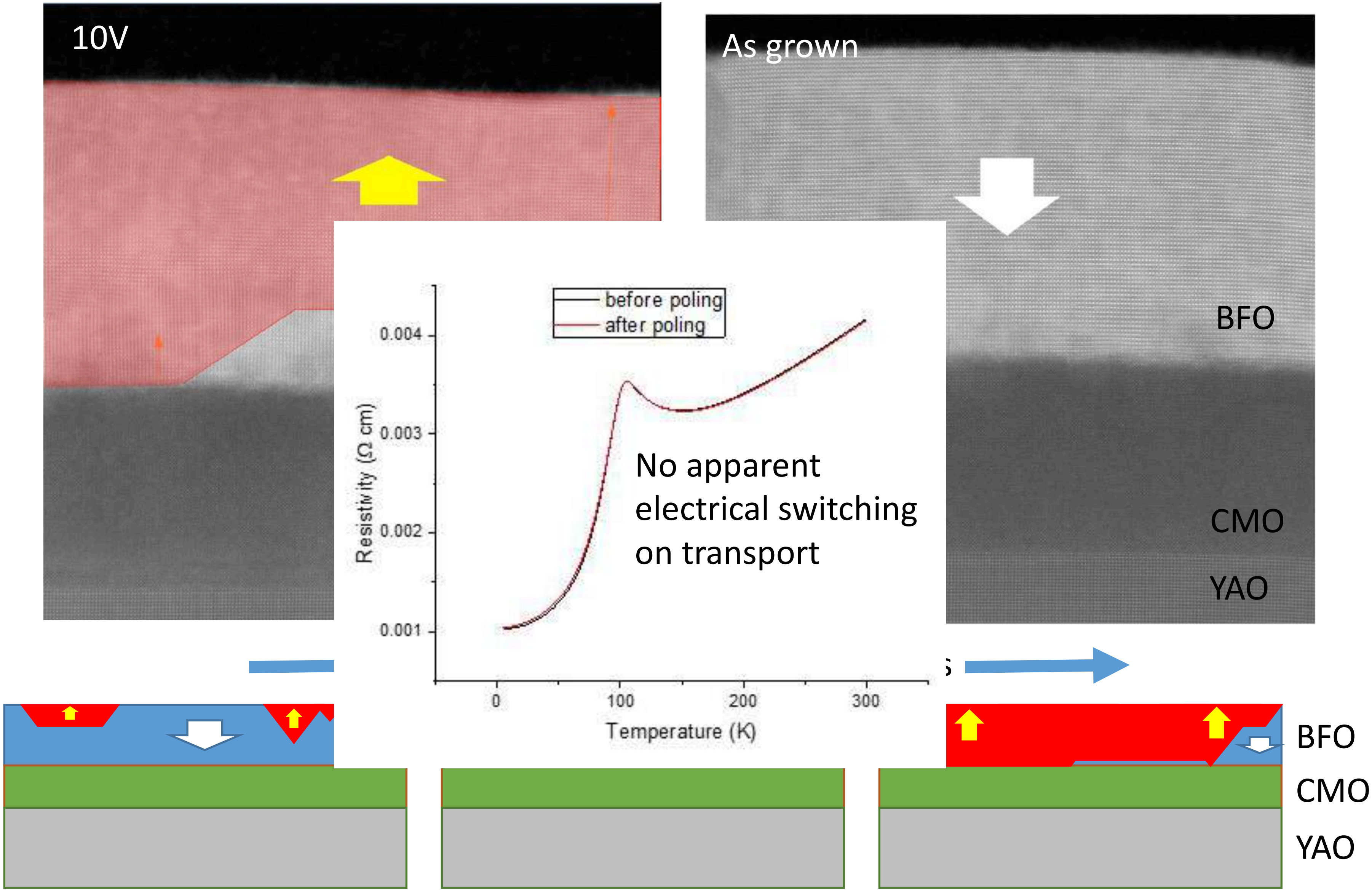
10V
As grown
BFO
CMO
YAO
before poling
after poling
Resistivity (Ω cm)
0.004
0.003
0.002
0.001
0
100
200
300
Temperature (K)
No apparent electrical switching on transport
BFO
CMO
YAO

Charges Ce doped CMO (EELS Mn $L_{2,3}$) for BFO pol-up and pol-dn

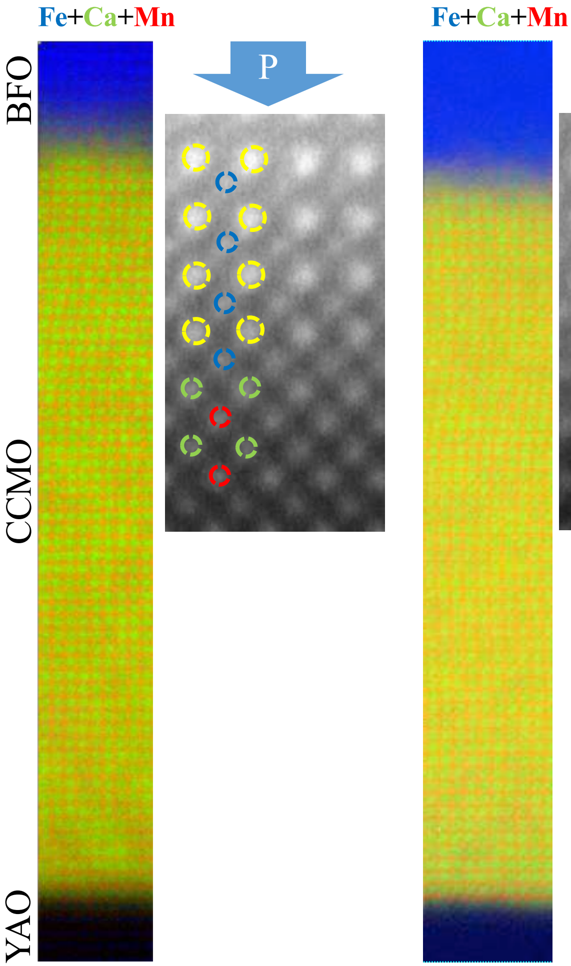

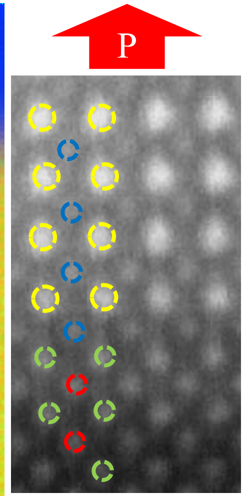

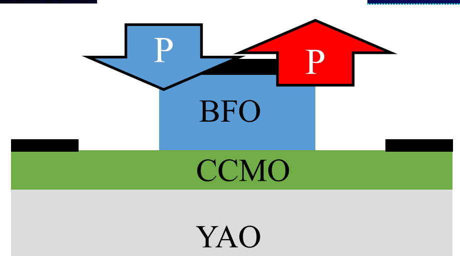

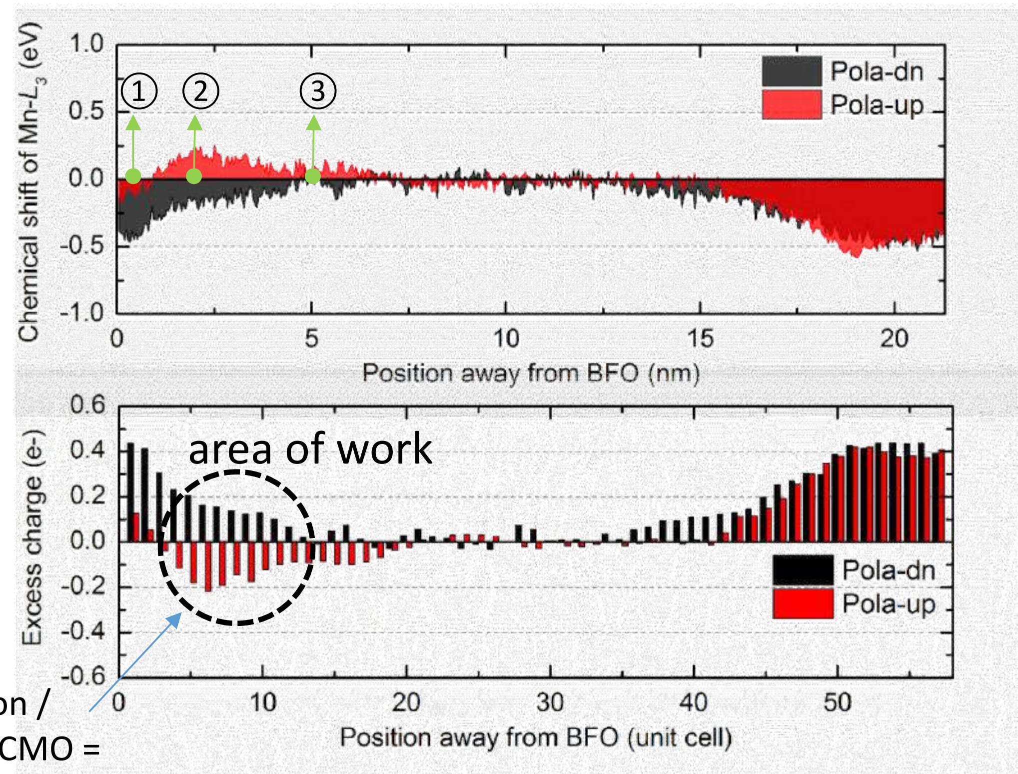

Charge accumulation / depletion at BFO/CCMO = electrostatic doping due to the ferroelectric polarization

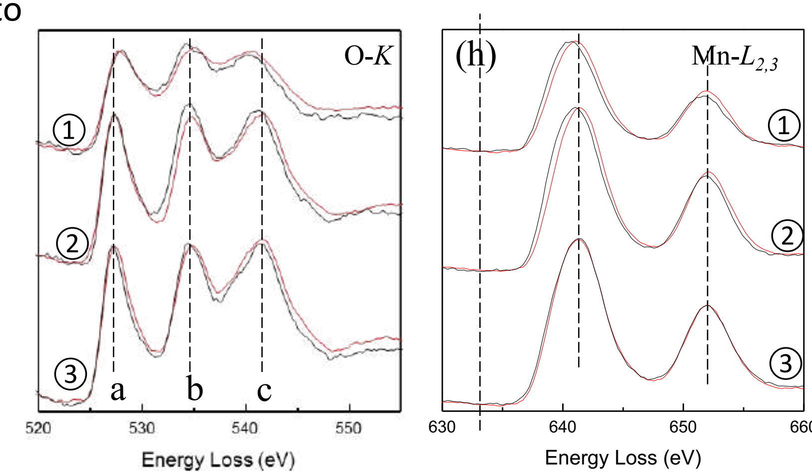

Orbitals hierarchy at the $LaAlO_3/SrTiO_3$ interface

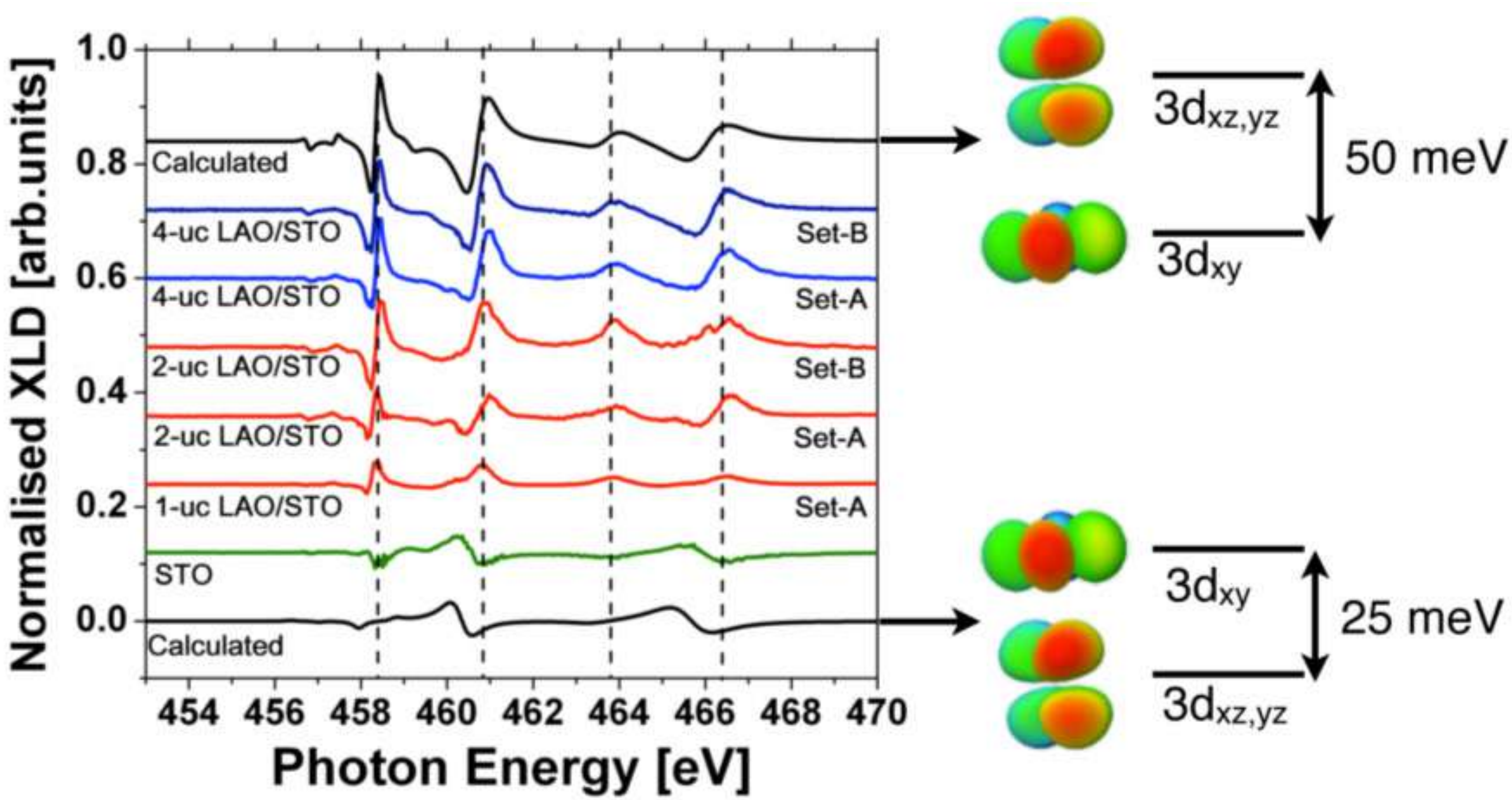

Figure 1. X-ray linear dichroism (XLD) spectra around the titanium $L_{2,3}$ absorption edge of $SrTiO_3$ (green line) and $LaAlO_3/SrTiO_3$ bilayers characterised by a $LaAlO_3$ thickness below (red lines) and above (blue lines) the critical thickness of four unit cells. Data from two sample sets are shown. Black lines are calculations which reproduce the data on STO (bottom) and LAO/STO (top) using multiplet atomic model calculations with point charge crystal field. On the right a schematic of the orbital splitting needed to reproduce the data is depicted, showing the inversion of hierarchy between in-plane and out-of-plane t_{2g} orbitals at the $LaAlO_3/SrTiO_3$ interface.

Salluzzo et al. PRL 102, 166804 (2009)

2D gaz are known to occur at $LaAlO_3/SrTiO_3$ interface

STO-substrate / LAO-f / STO-f / LAO-f

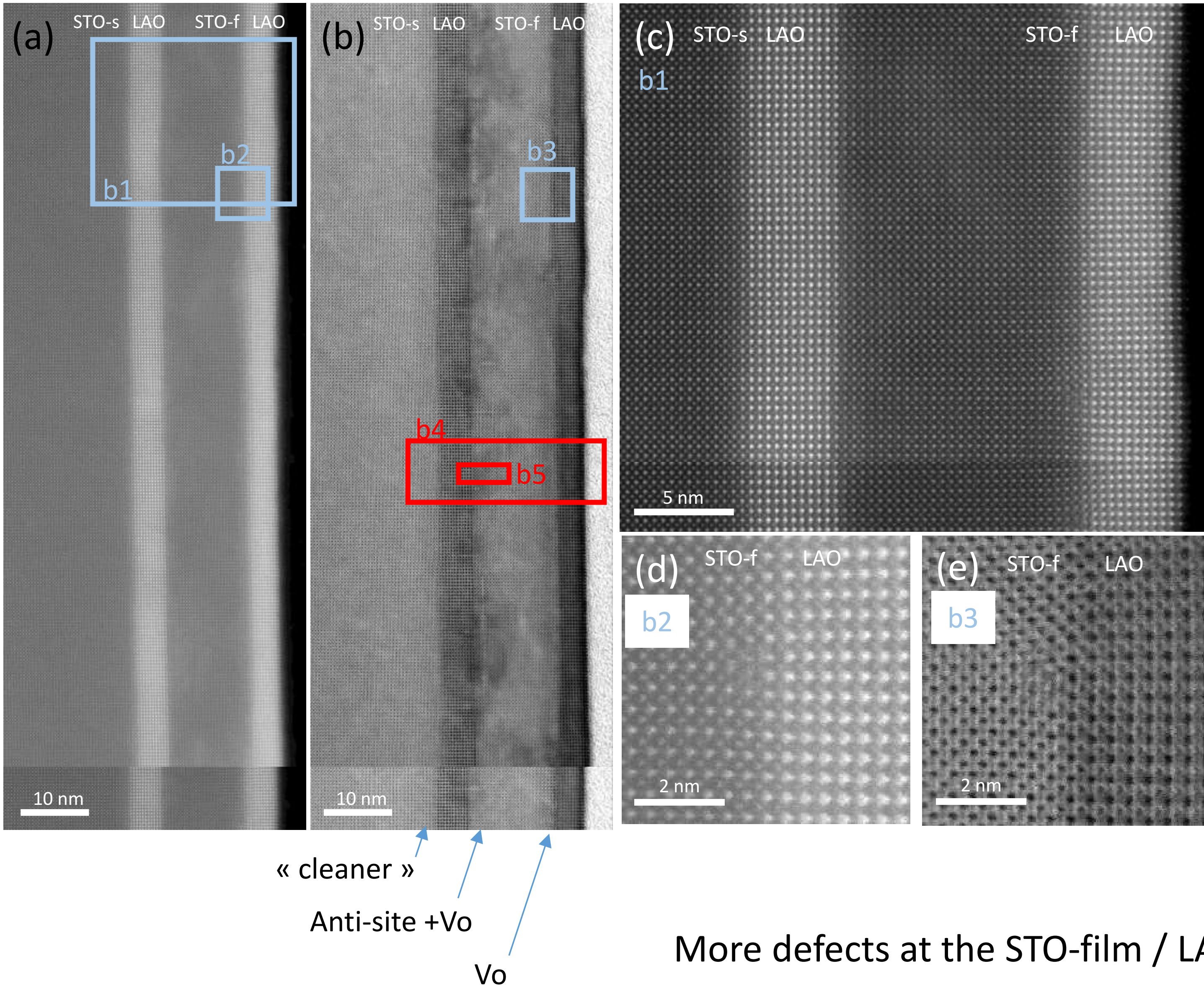

Coll. JM. Triscone (U. Geneva)

G. Tieri et al. submitted

More defects at the STO-film / LAO-film interfaces

Interface plane terminaison by elemental EELS mapping

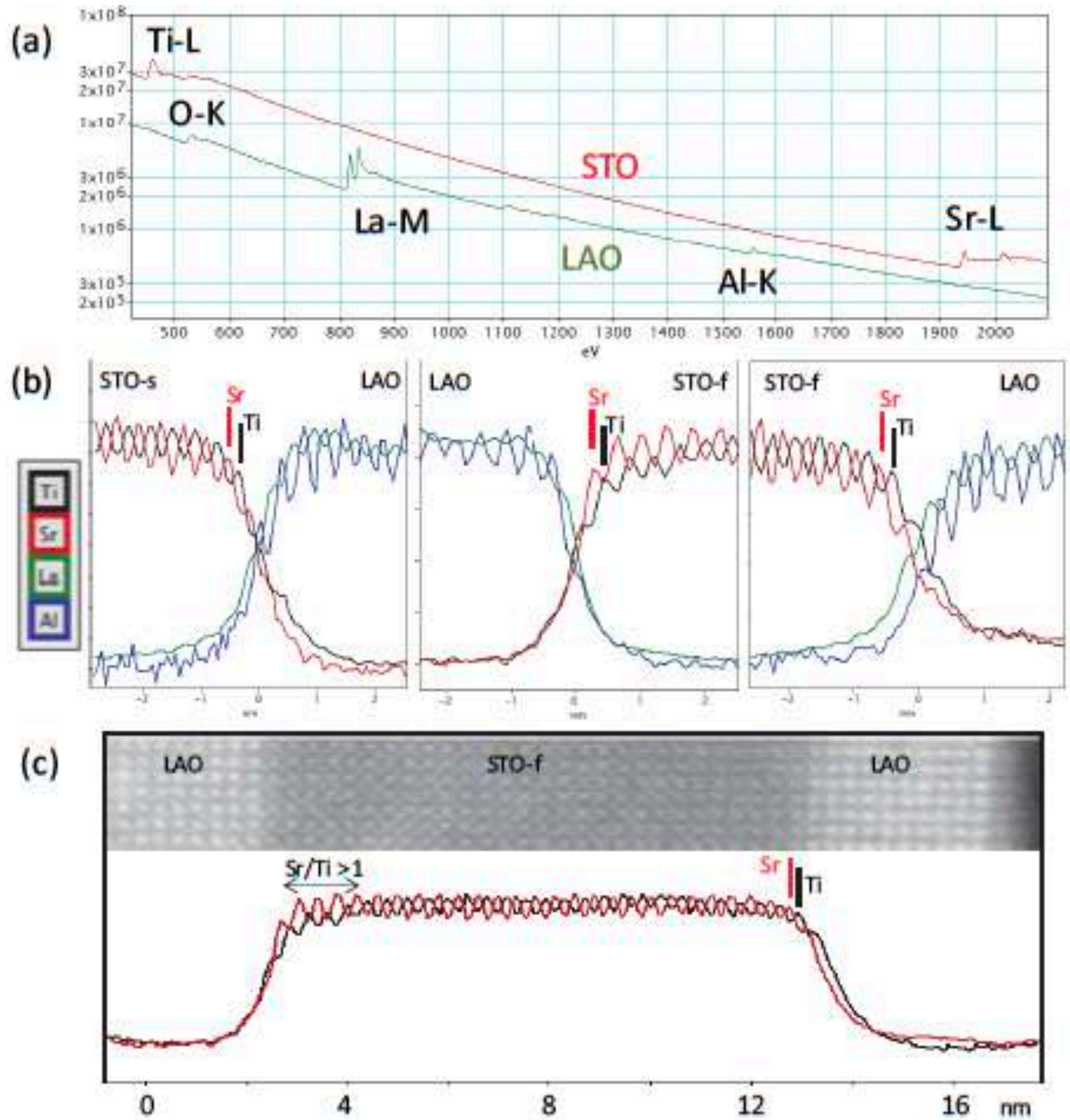

Defects and off stoechiometry

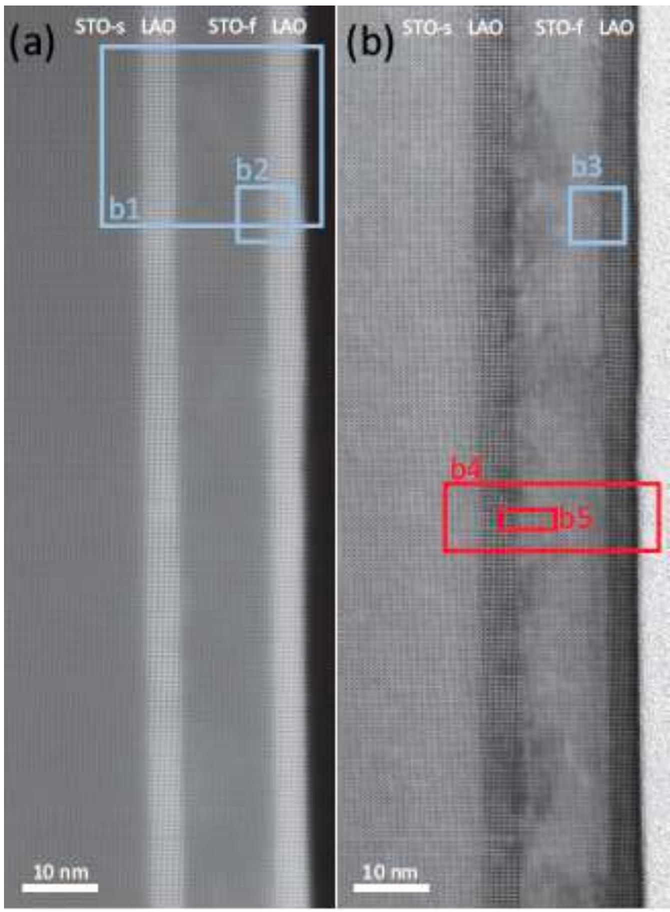

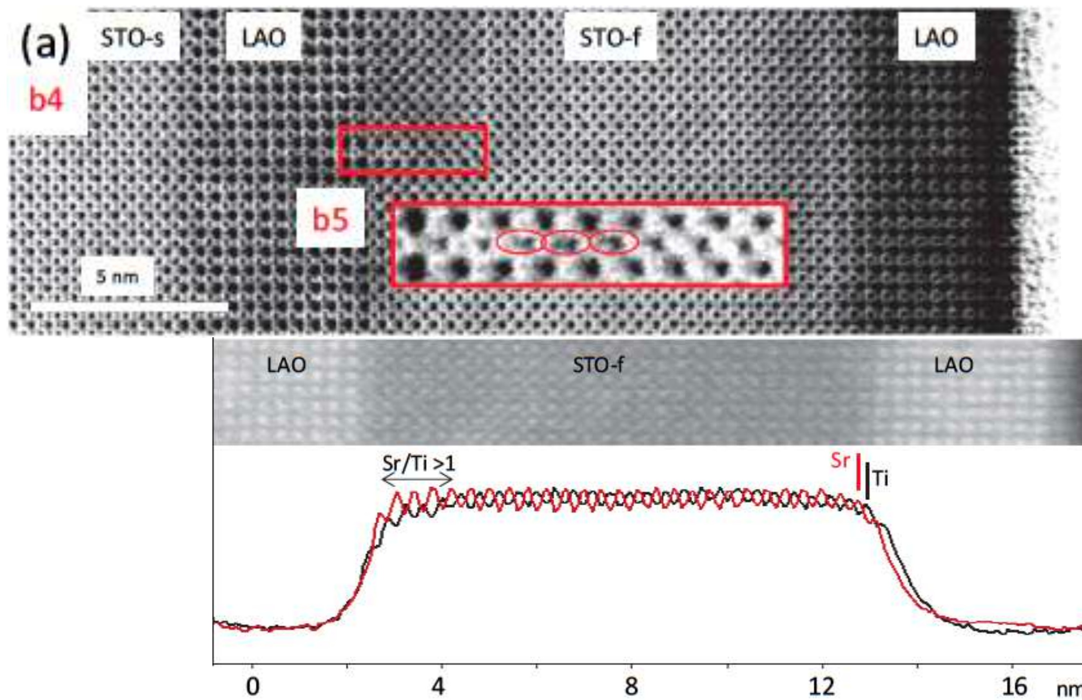

Sr antisites

Oxygen vacancies?

Mapping and quantifying Ti^{3+} states

Spectroscopic quantification of additional electrons at the interfaces

STO-s/LAO: higher Ti^{3+} and higher confinement

STO-s/LAO: lower Ti^{3+} content, larger spatial extension

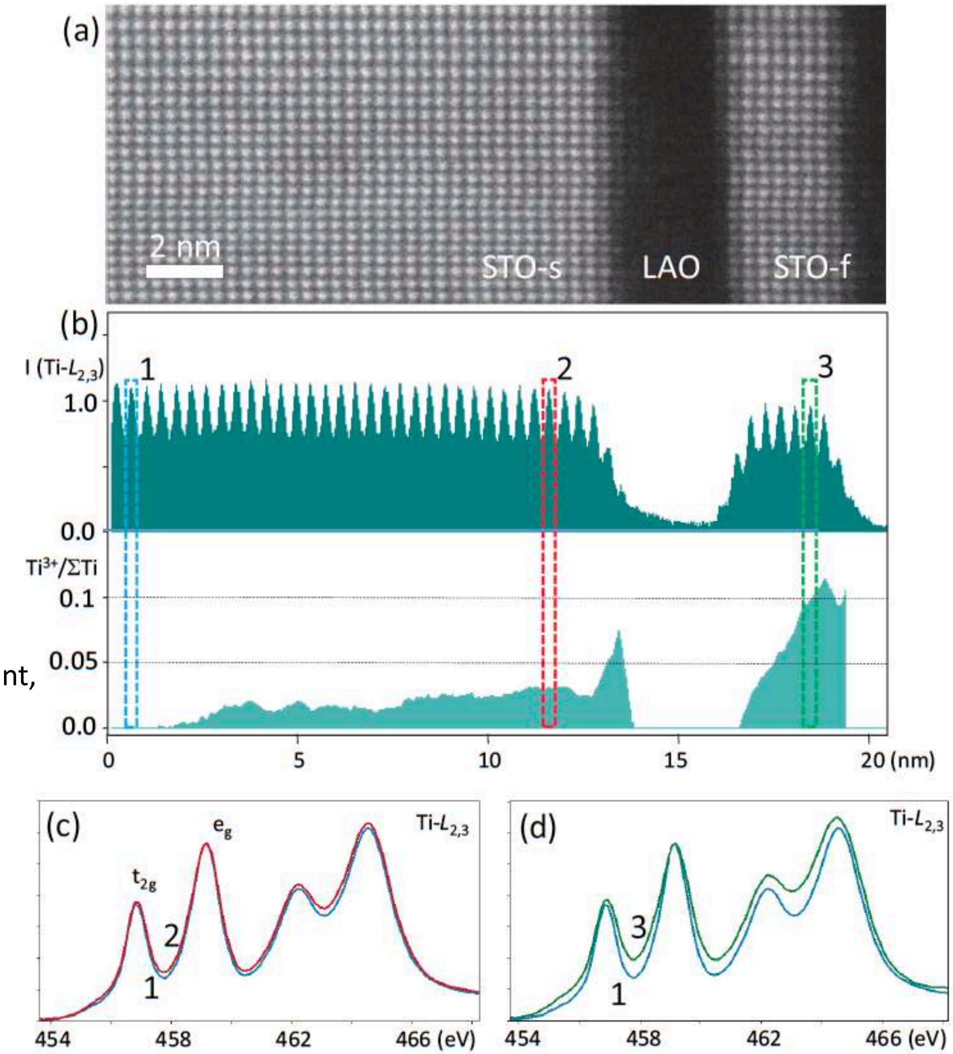

STO-s/LAO: 0.03 Ti^{3+}

STO-f/LAO: 0.1 Ti^{3+}

Typical (spectroscopic) total charge: 0.5-0.6 e-

This is significantly higher than expected for the transport carrier densities, indicating that a significant amount of the carriers at these interfaces are localized

Spectroscopic probing of Ti^{3+} states by XAS and resonant PES

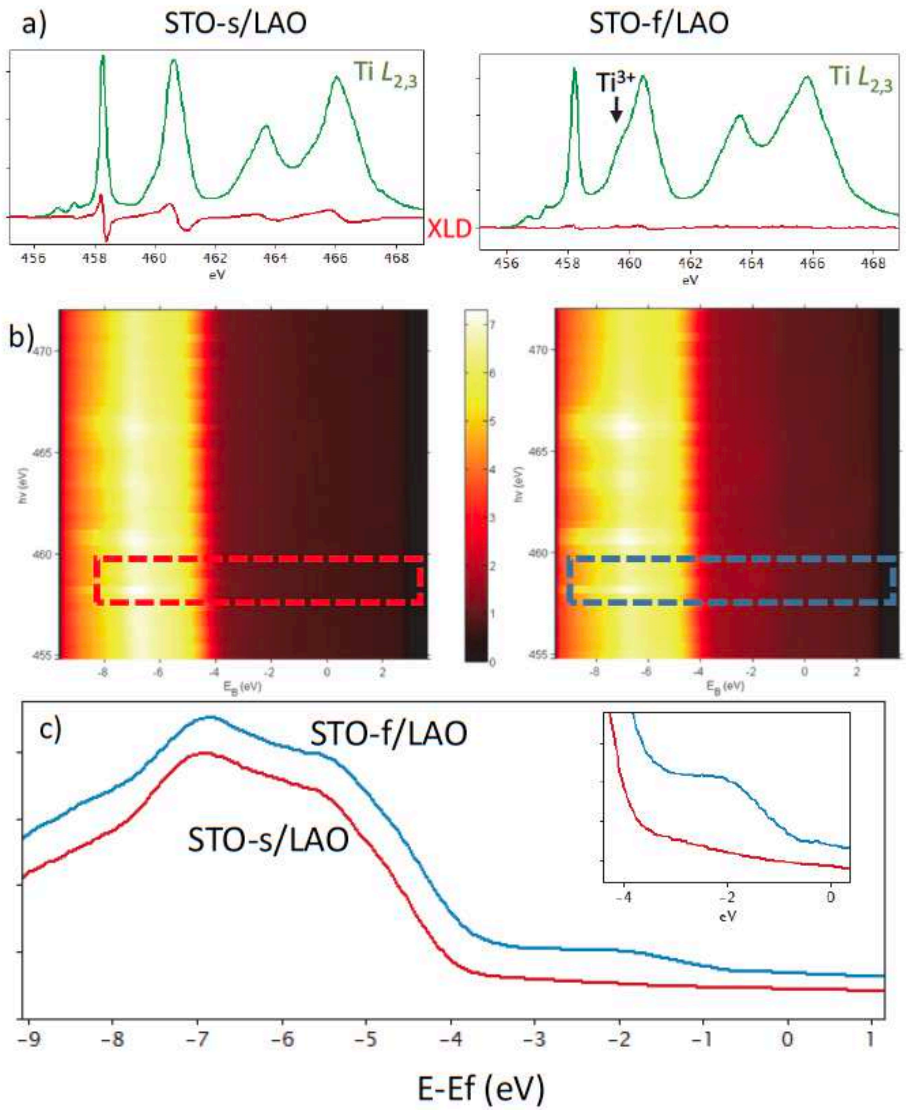

Larger Ti3+ signature at the STO-f/LAO interface

In gap states (charged V_O states?) at the STO-f/LAO interface

Coll. V. Strocov (SLS)

XLD Ti L2,3 for both interfaces

Intense dichroïc signal at the STO-s/LAO whose sign confirms that the $3d_{xy}$ orbital lies at lower energy

STO-s/LAO

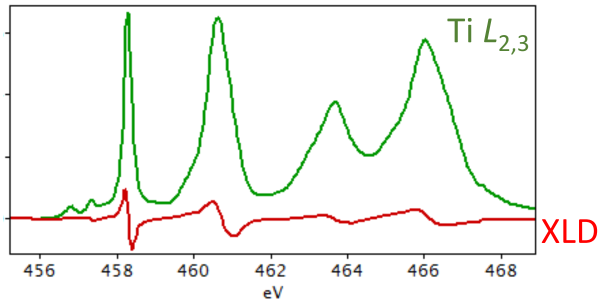

STO-f/LAO

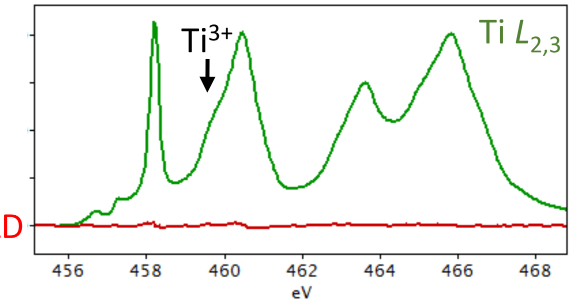

No dichroïc signal for the STO-f/LAO interface indicating that the orbital hierarchy is supressed (or blurred)

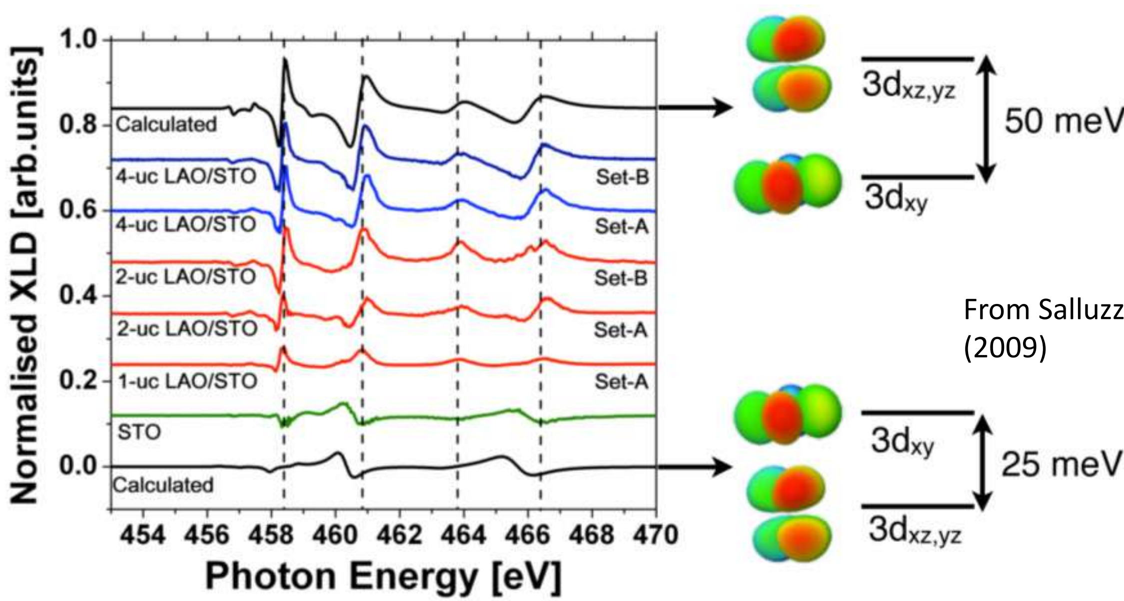

From Salluzzo et al. PRL 102, 166804 (2009)

Different orbitals hierarchy at the different $LaAlO_3/SrTiO_3$ interfaces of the bi-layer ?

Isotropic EELS Ti $L_{2,3}$ for both interfaces

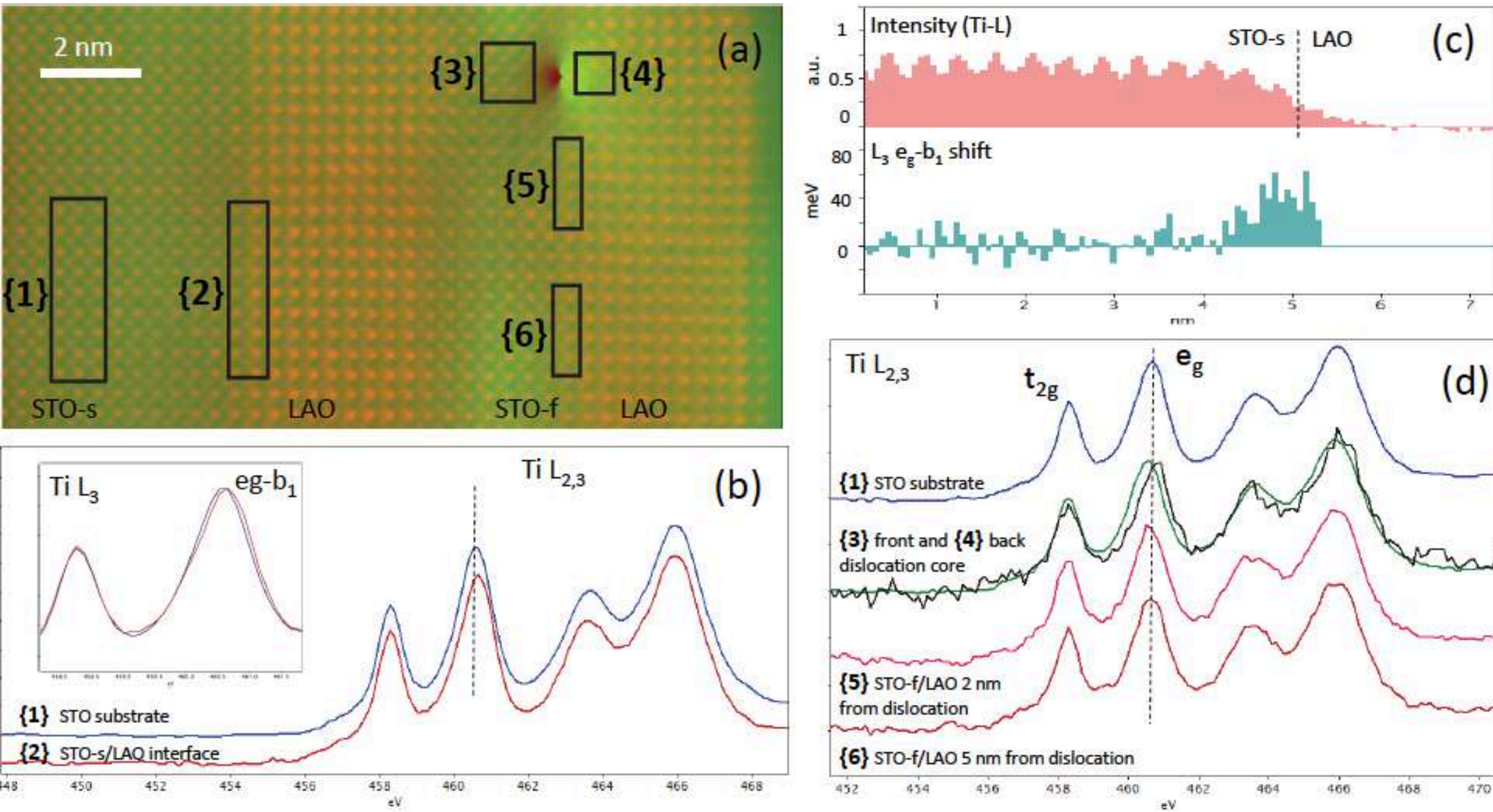

Different orbitals hierarchy at the different $LaAlO_3/SrTiO_3$ interfaces of the bi-layer ?

Orbital ordering in LAO/STO bilayers

XAS isotropic and EELS comparison Ti L on LAO-STO

STO (substrate) / LAO

STO / LAO

G. Tieri et al. submitted

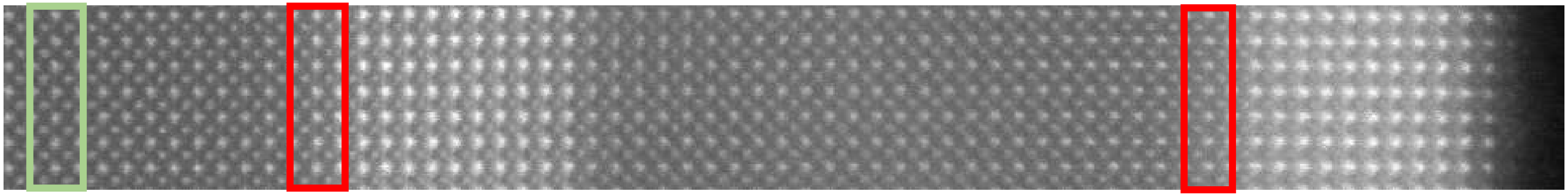

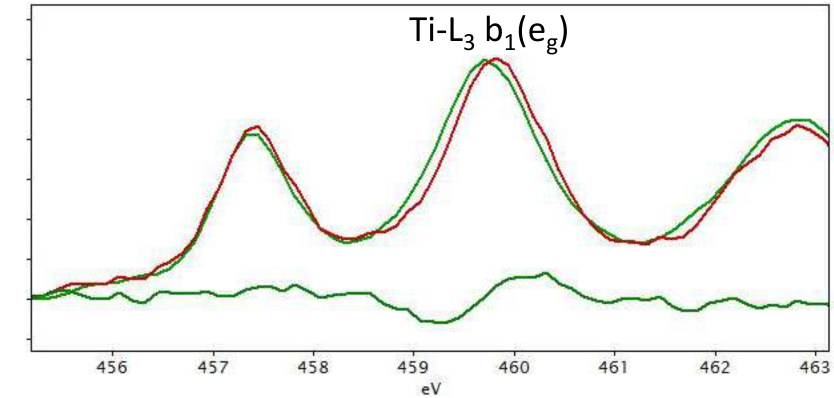

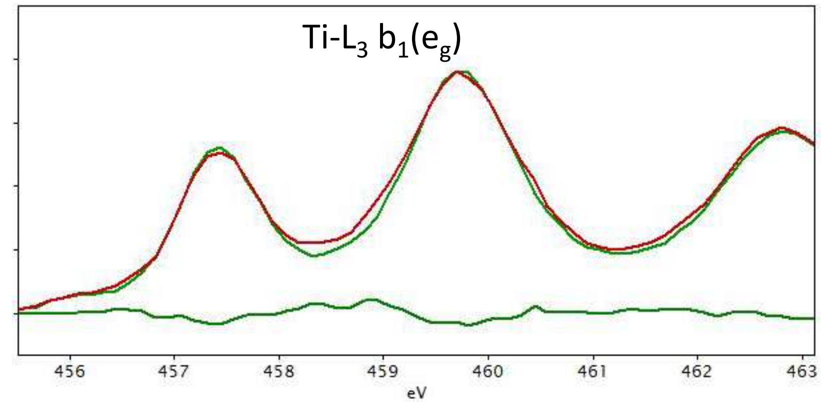

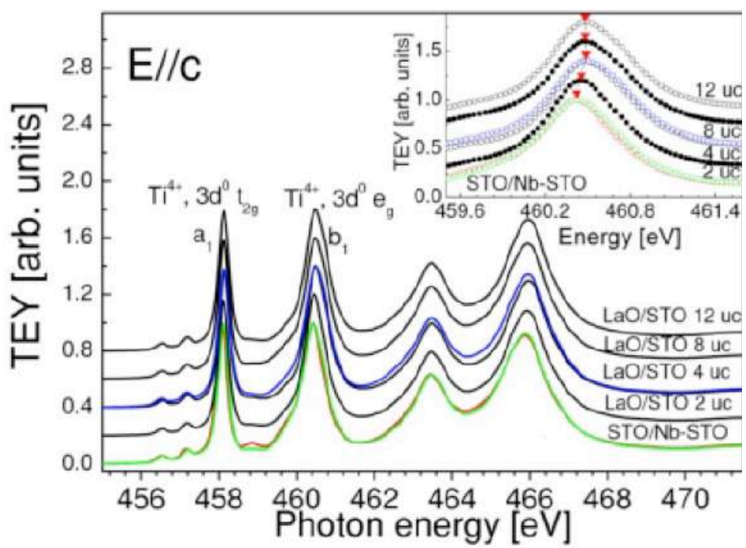

From Salluzzo et al. PRL 102, 166804 (2009)

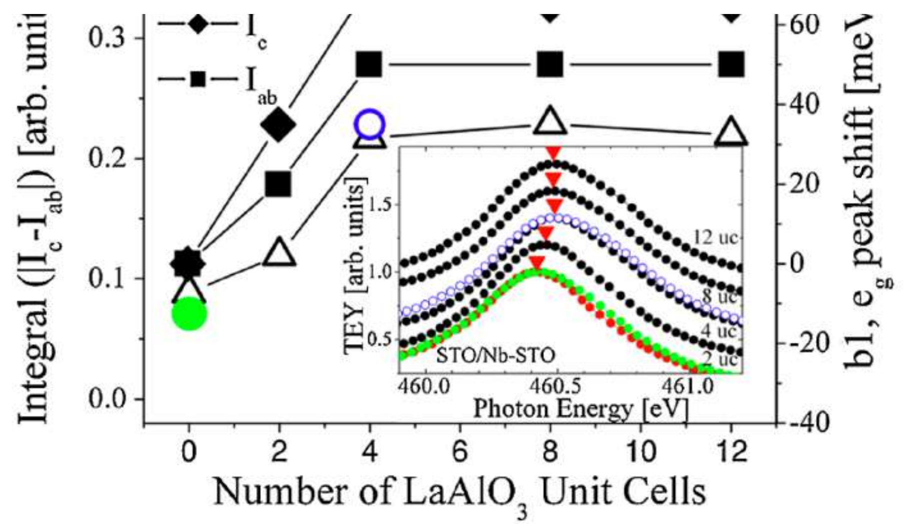

PRL **102,** 166804 (2009) PHYSICAL RE

Real space extension of the « strong » orbital polarisation

STEM-EELS

50 meV L3 eg shift is only measured for the Ti @ interface : SrO – TiO2 - LaO

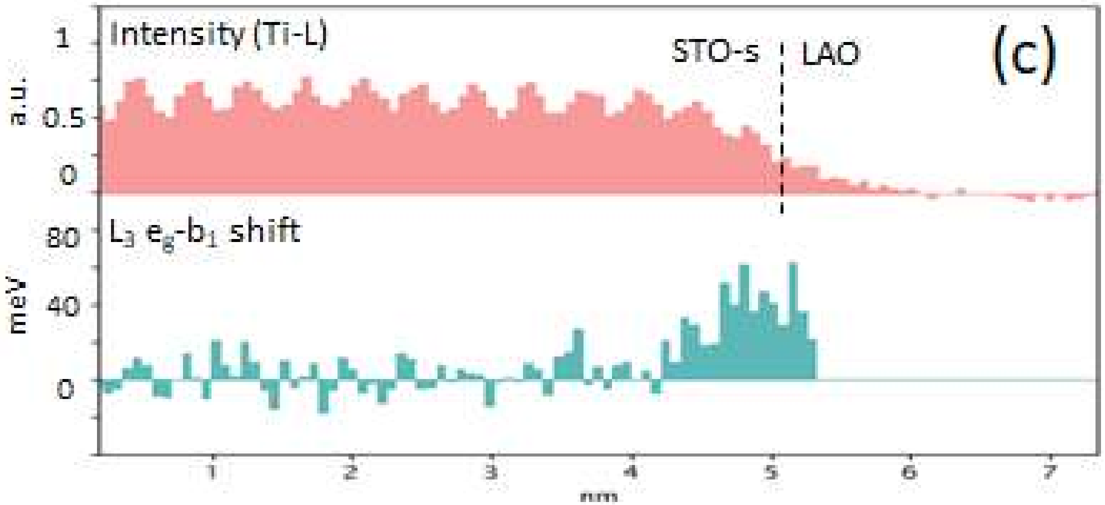

G. Tieri et al. submitted

Ab-initio

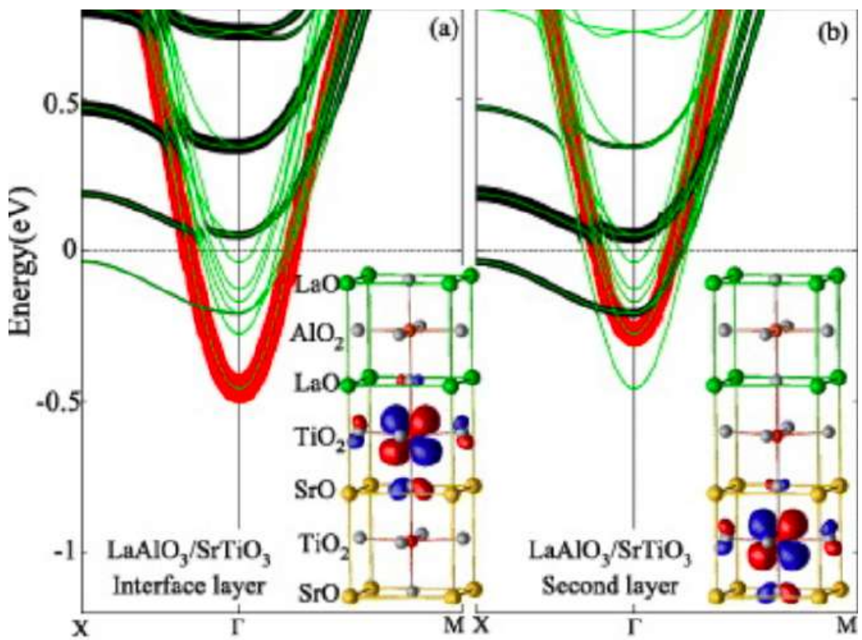

From Zhong et al., EPL 99 (2012) 37011

1) Octahedra rotation in $LSMO_3/STO_3$ superlattices

2) Charge control in manganite by ferroelectric switching in $CaMnO_3/BiFeO_3$ based Mott transistor.

3) Orbital ordering in $LaAlO_3/SrTiO_3$ bilayers

4) Low energy excitation in ABO_3 (B=TM) by EELS

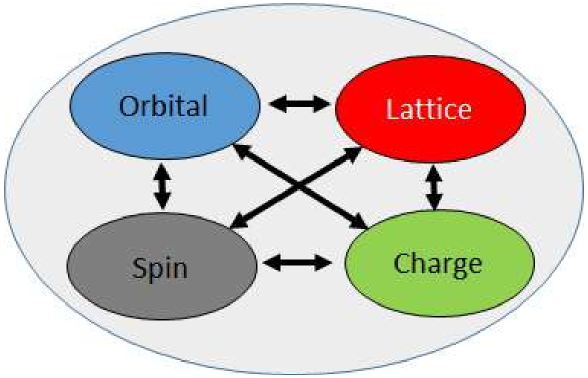

Higher spectral resolution STEM-EELS (keeping sub-nanometer spatial resolution)

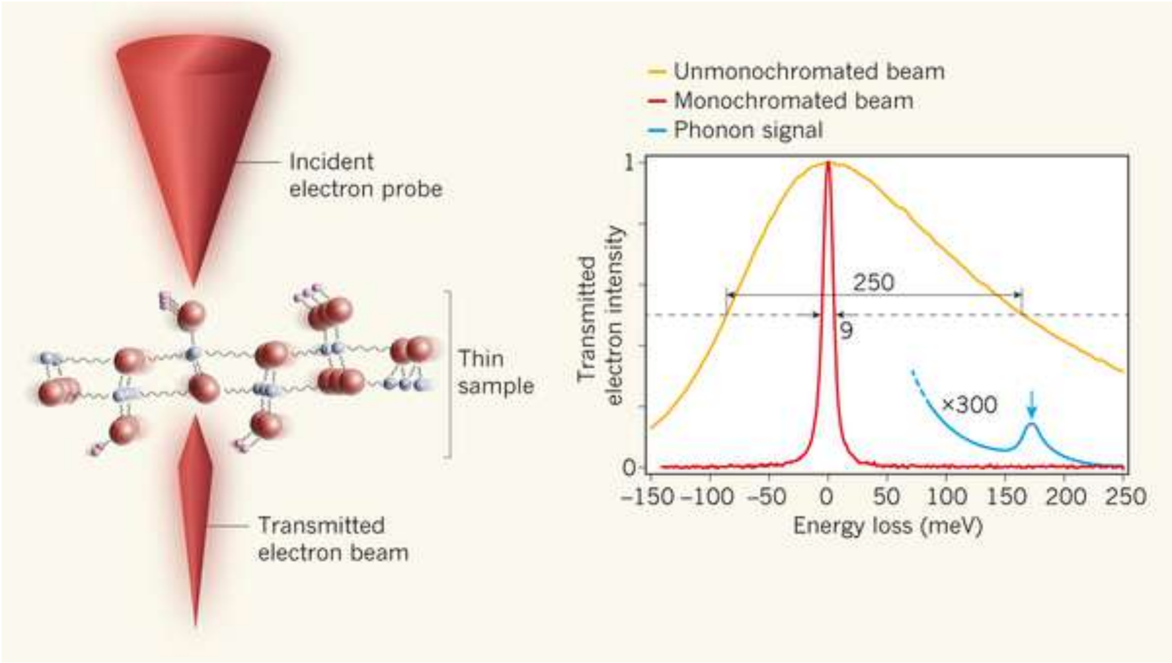

LO phonon in h-BN, with a peak energy of 173meV

Krivanek et al. Nature **514**, 209 (2014).

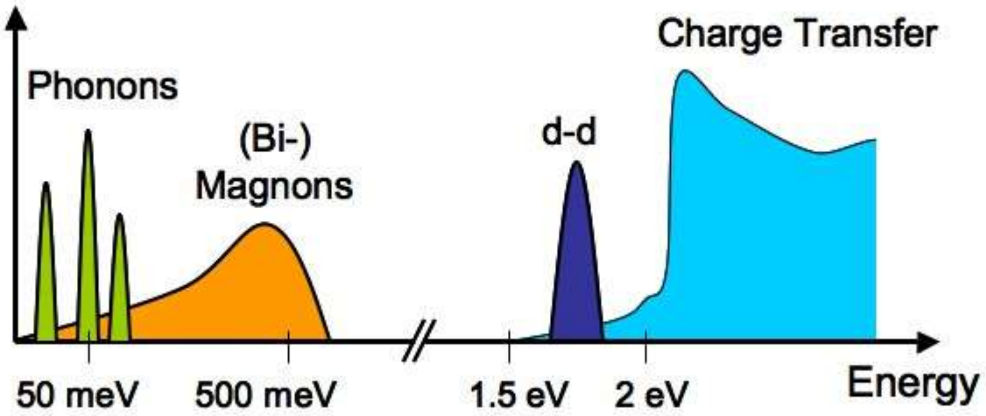

Few perspectives

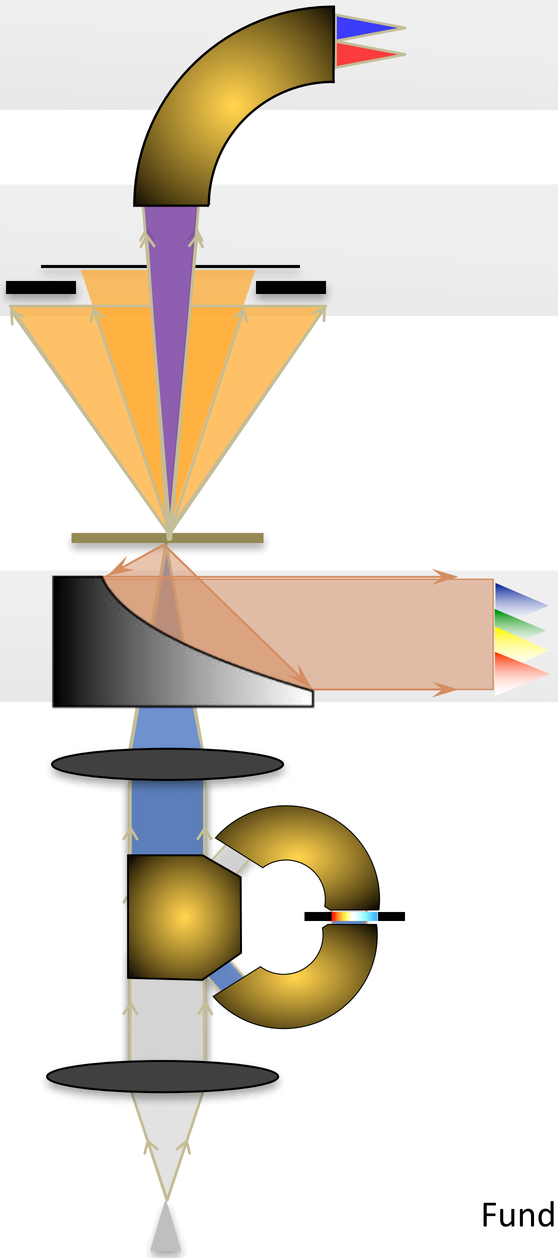

	“A synchrotron in a STEM”	Optical bench in a STEM
High resolution **EELS**	50 -100 meV	5 meV
High Resolution **imaging**	1 Å	Sub-nm
Low temperature (He & N_2)		
NanoCL & **Light** injection		1 meV
High currents	60 pA	10 pA @ 10 meV (50 pA @ 50 meV)
High resolution **monochromation**		

Other specs, especially for reciprocal space measurements

Funded in 2010

INVESTISSEMENTS D'AVENIR

Equipement d'excellence TEMPOS

Transmission Electron Microscopy at Palaiseau Orsay Saclay

The CHROMATEM microscope

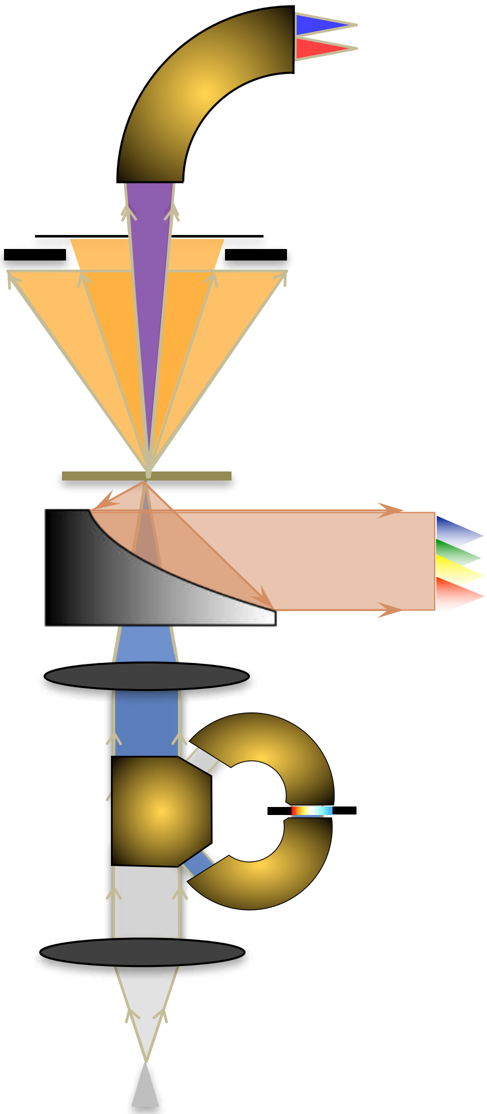

- NION Hermes 200M
- 30-200 kV
- Side entry stage
- High-resolution EELS spectrometer

- HennyZ sample holders:
- Variable temperature (LN_2-600°C)
- Electrical contacts

- Attolight light injection/detection system

Delivery early 2018

CHROMATEM: providing a priviledged access to very low losses down to the IR

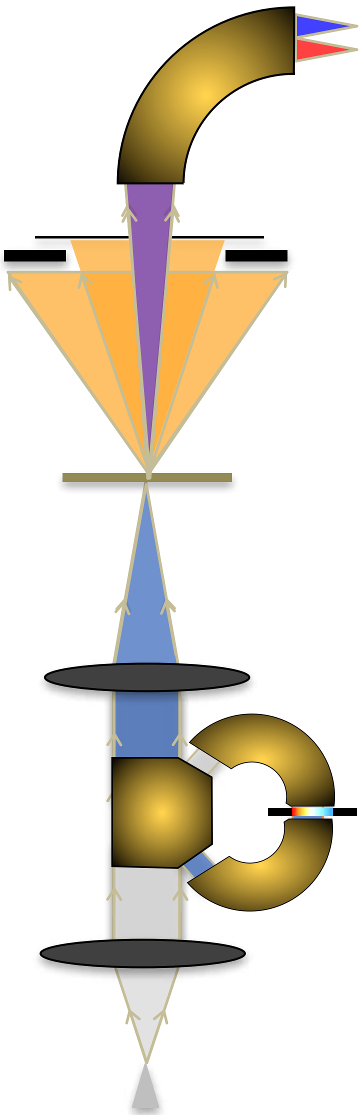

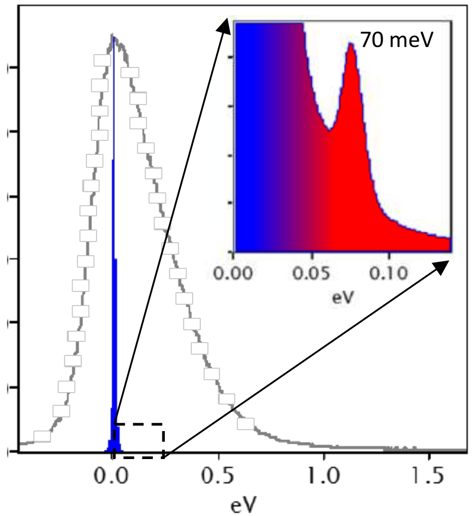

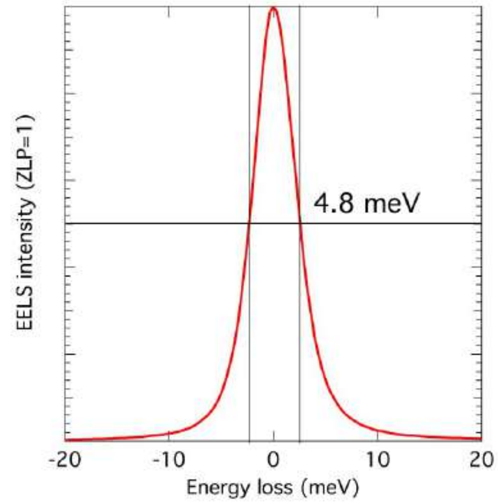

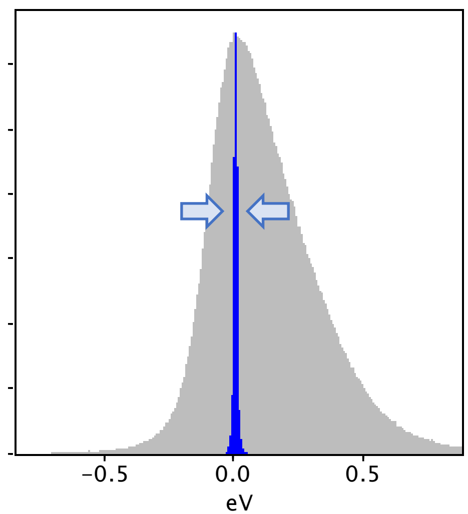

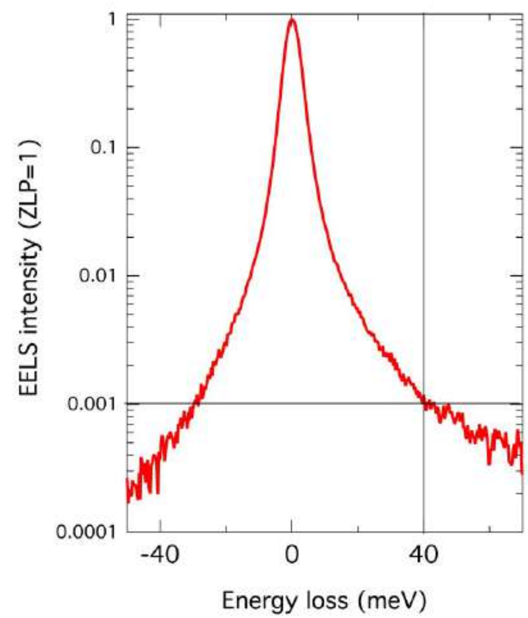

“Classical” localized plasmons are now routinely mapped by STEM –EELS or STEM CL

A very lively field
Wherever space and energy variations are entangled

Nelayah, J. et al. Nat. Physics (2007)
Vesseur, E. J. R., et al. Nano Lett. 7, 2843–2846 (2007).
Gu, L. et al. Phys. Rev. B 83, (2011).
Nelayah, J. et al. Nano Lett. 10, 902–907 (2010).
Rossouw, et al. Nano Lett. 11, 1499–1504 (2011).

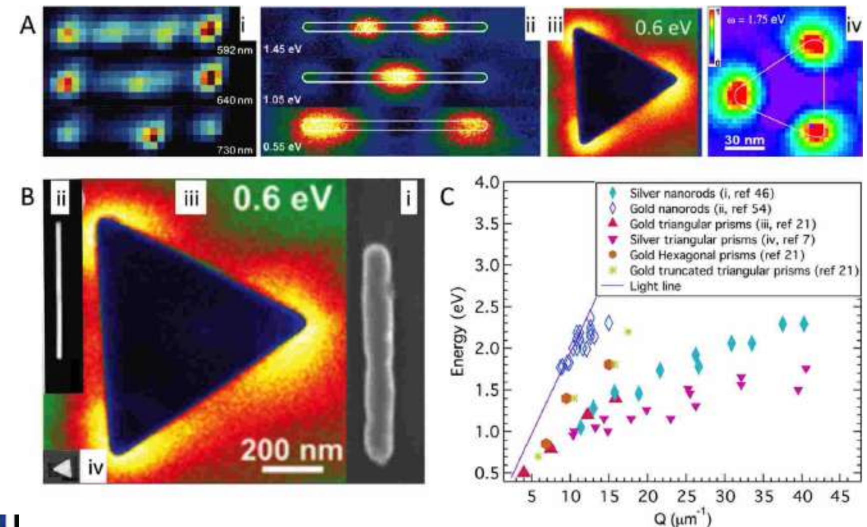

Plasmon classification

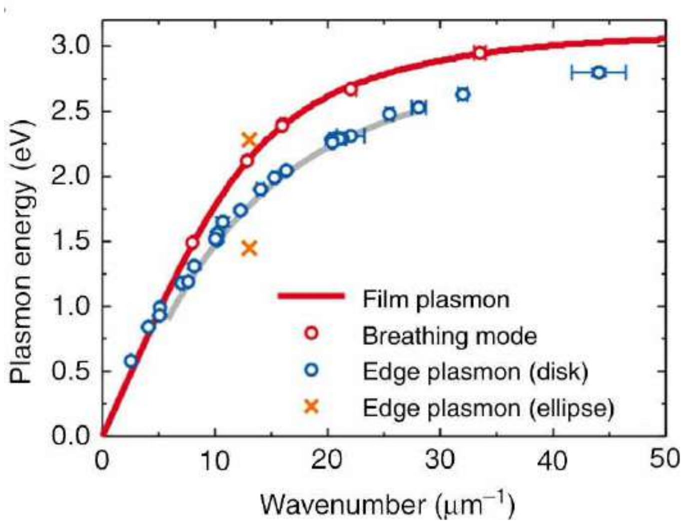

Schmidt, F.-P. et al. Nature Communications 5, (2014).

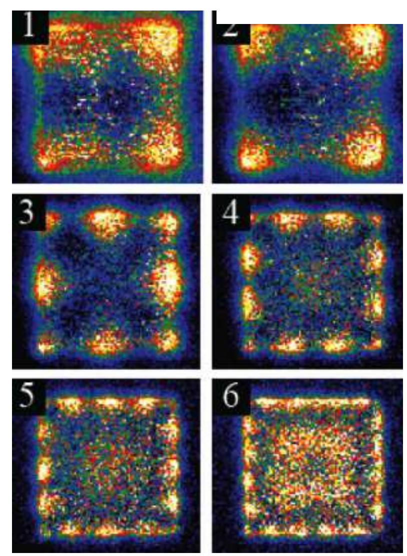

Bellido et al. ACS Phot. (2016)

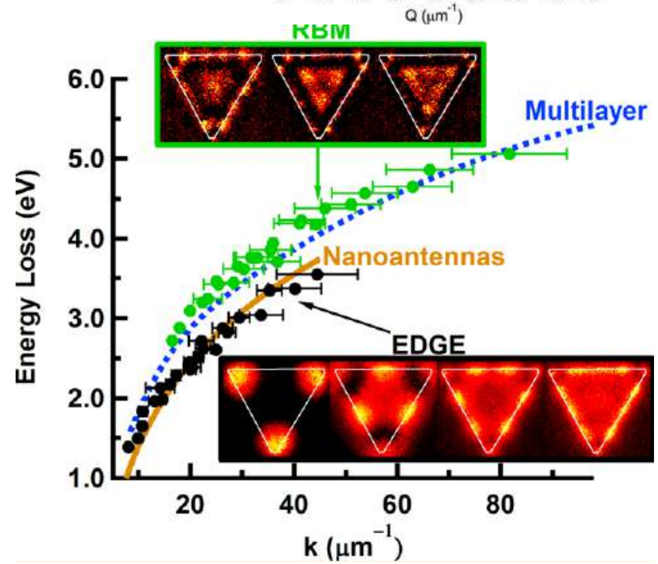

Campos et al. ACS Phot. (2017)

Spatially resolved low energy excitation
THz plasmons: the example of plasmon modes in a Cu nanowire

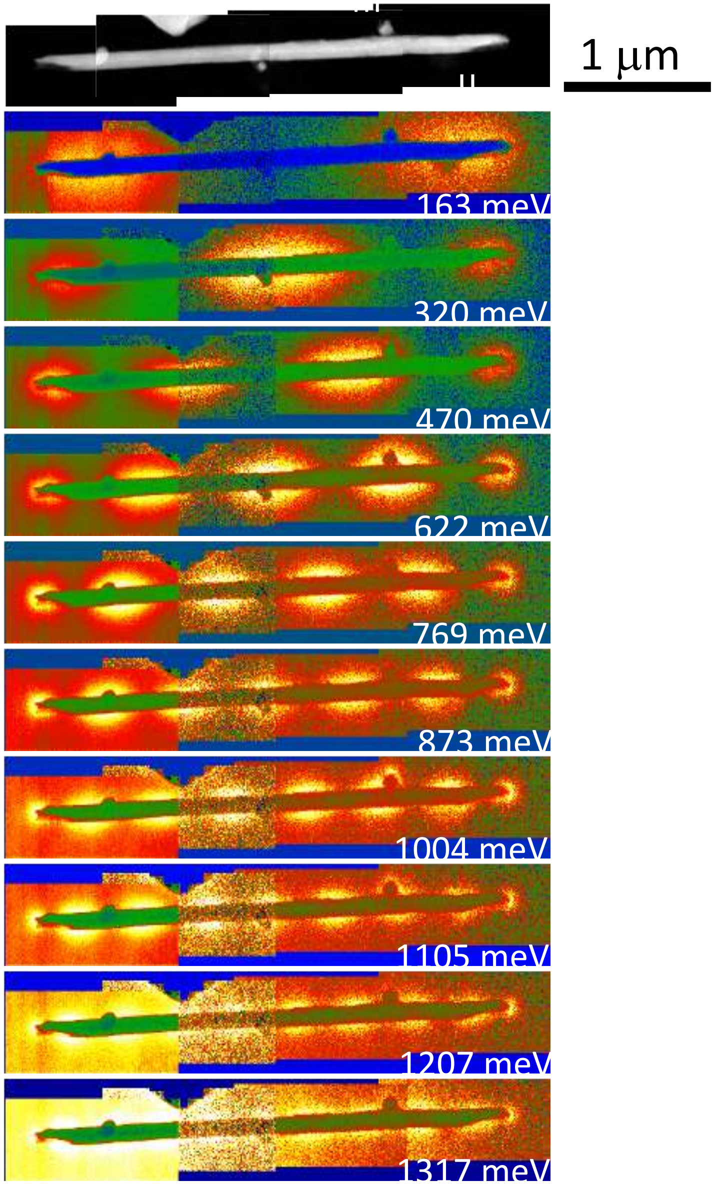

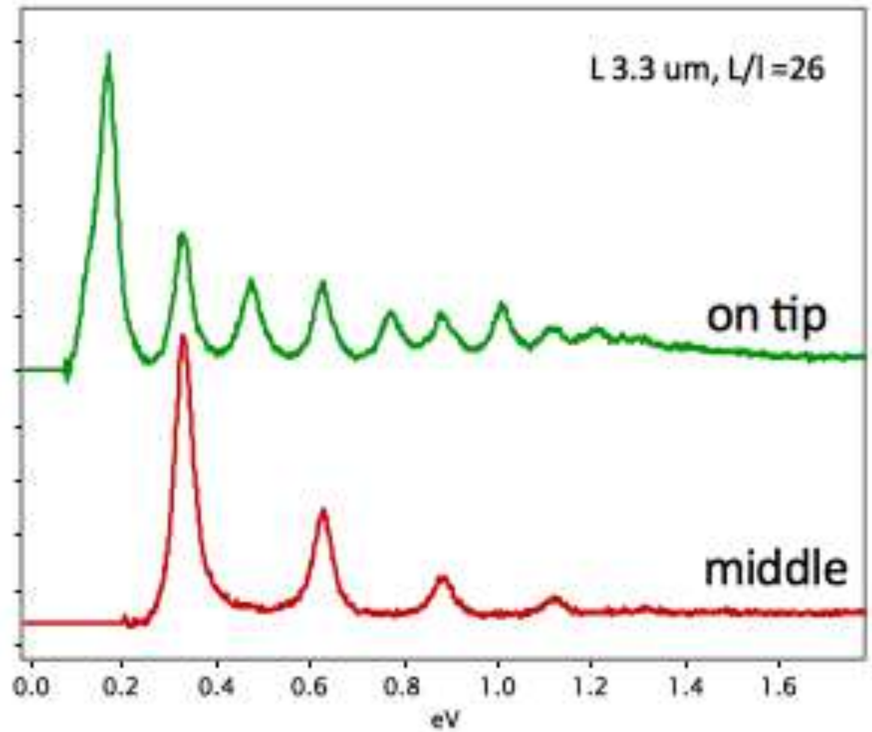

A. Gloter,
M. Kociak (LPS-Orsay)
SY Chen (NTUST)
S. Song (NCHU)
Unpublished

EELS in CHROMATEM microscope -> down to 5 meV energy resolution @ 30 keV

- Plasmon modes on « long » metallic nano-rods

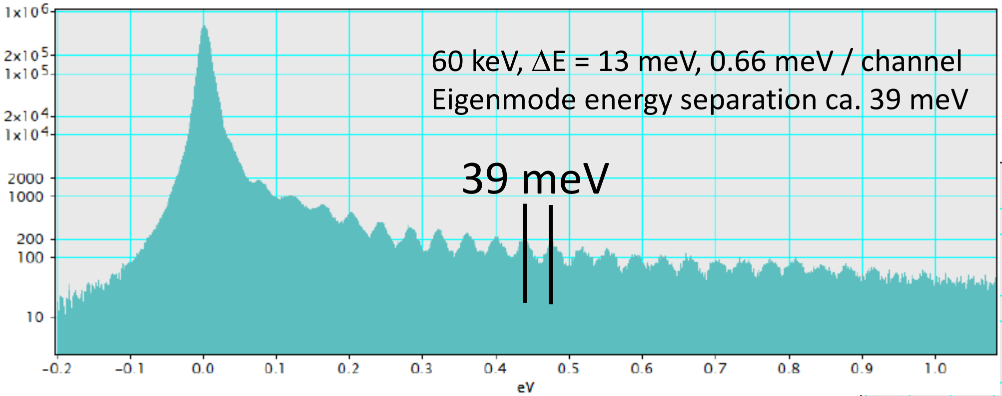

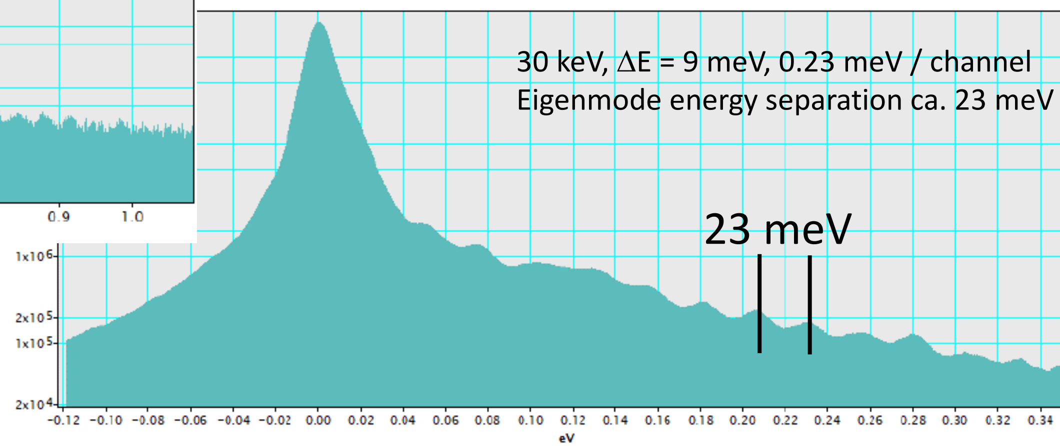

E. Tseng, A. Gloter, L. Tizei, X. Li, O. Stéphan, M. Kociak and NTUST-TW collaborators (in preparation 2019)

- « TMO oxides »

Access (*and map with nanometer scale resolution !!!)* the low energy electronic excitations in transition-metal oxide based nanostructures

Phonons, magnons ??, d-d, p-d, plasmons

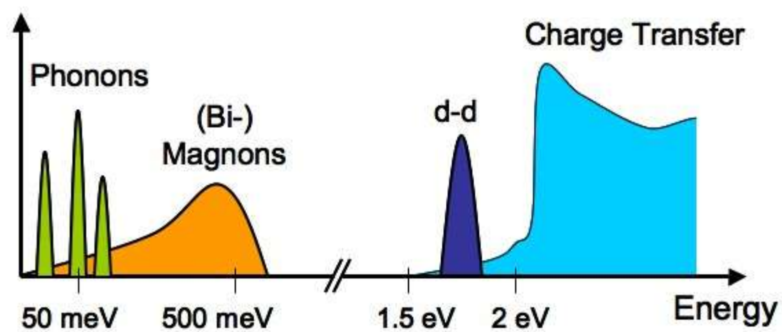

Ament et al. Rev. Mod. Phys.,83, 2011
RIXS review

MIT transitions at the nanoscale: V_2O_3 as an archetypal MIT system

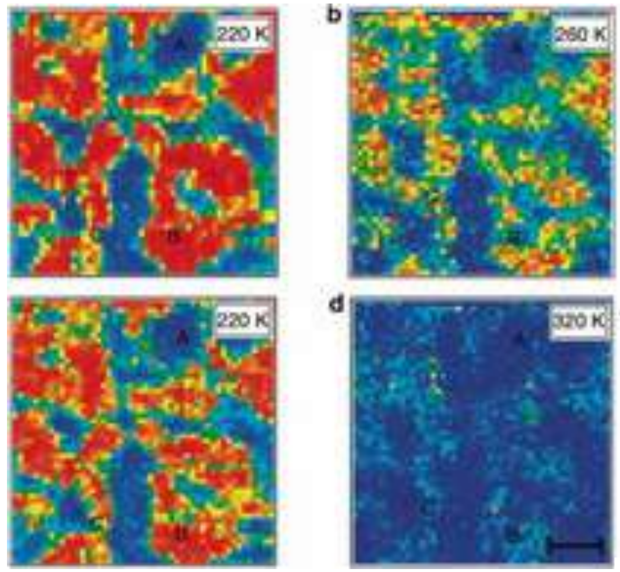

MIT in the V_2O_3 thin films at 137 K

Lupi, S. *et al*. *Nature Communications* **1,** 105 (2010).

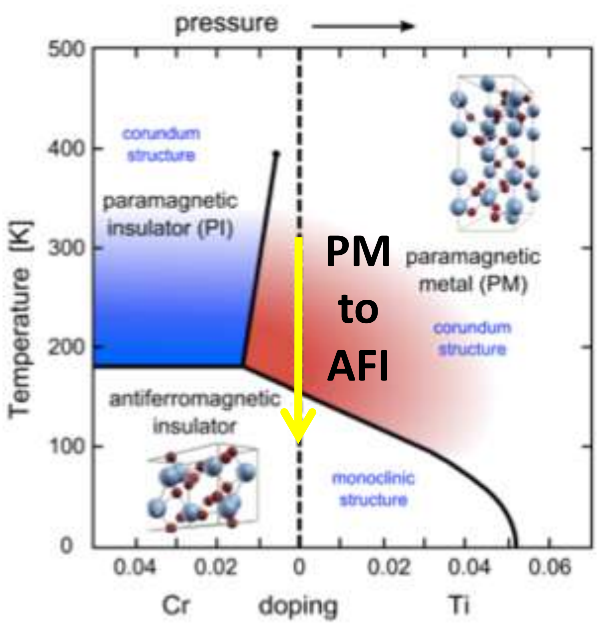

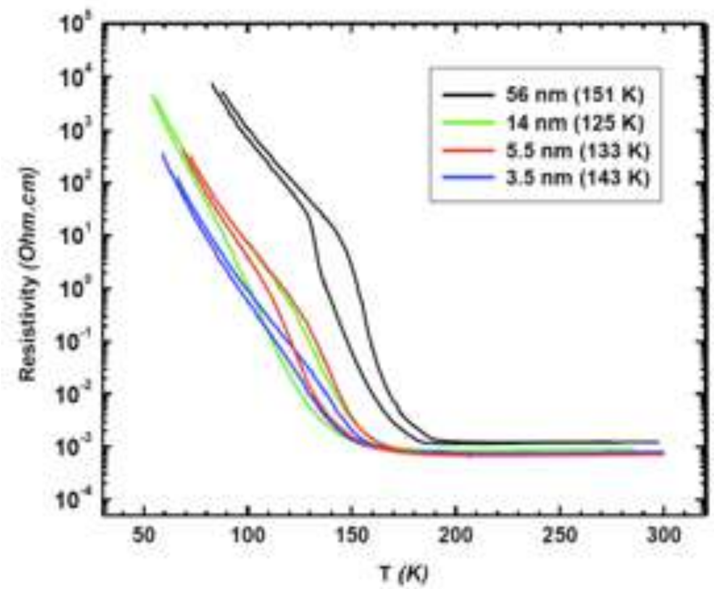

L. Dillemans et al. APL 104 (2014) 071902

Thermally-induced metal-insulator transition
Core-loss excitations probed through the low-T MIT

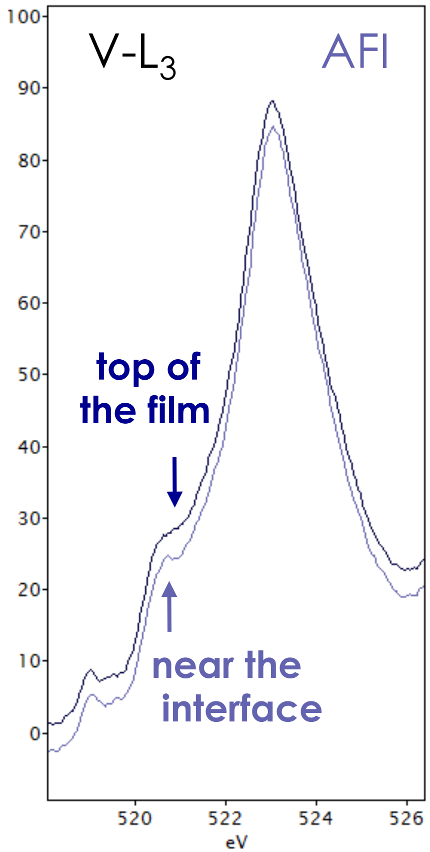

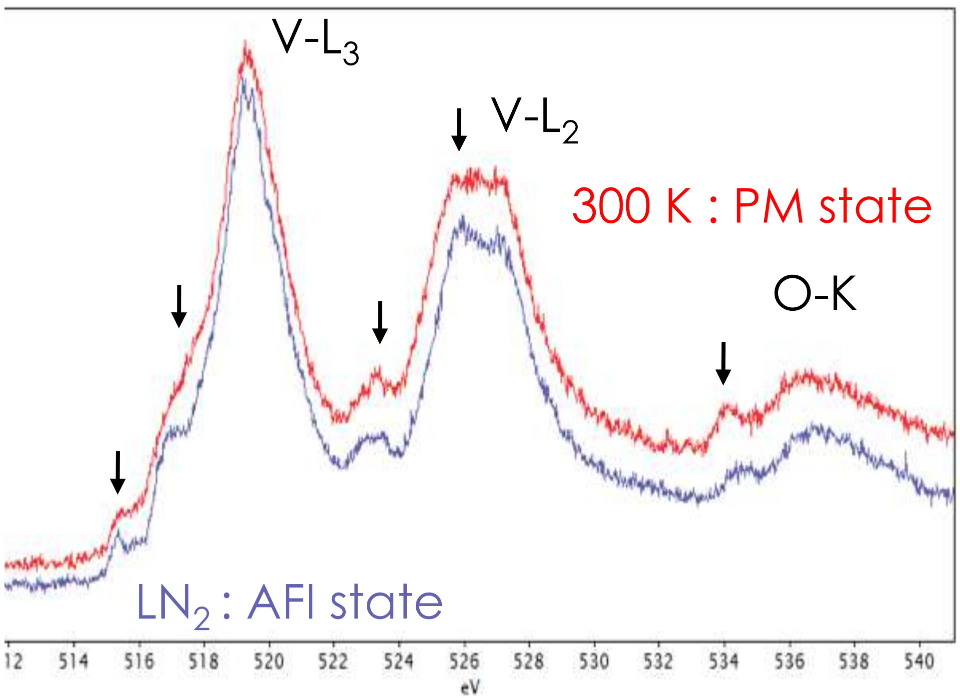

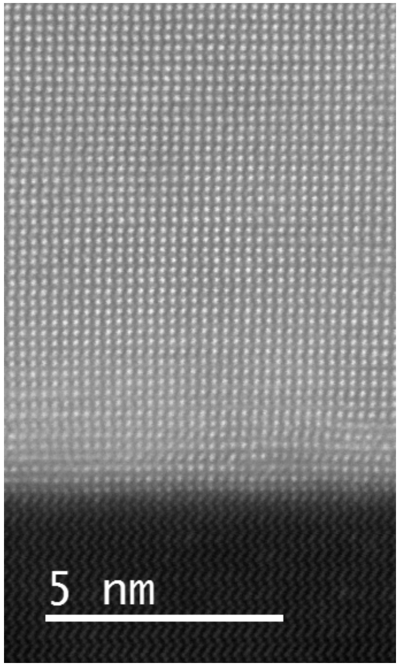

L. Bocher & X. Li, unpublished (2018)
Coll. M. Menghini et al. KU Leuven
See Laura Bocher's talk tomorrow

➔ PM and AFI spectroscopic signatures as in Abe et al. JJAP 38 (1999)

Mapping the metallic state

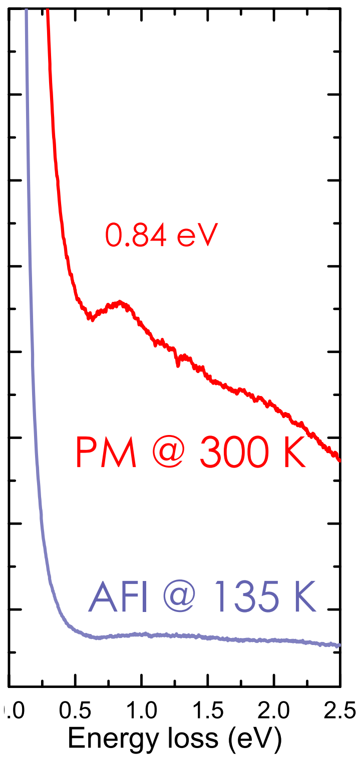

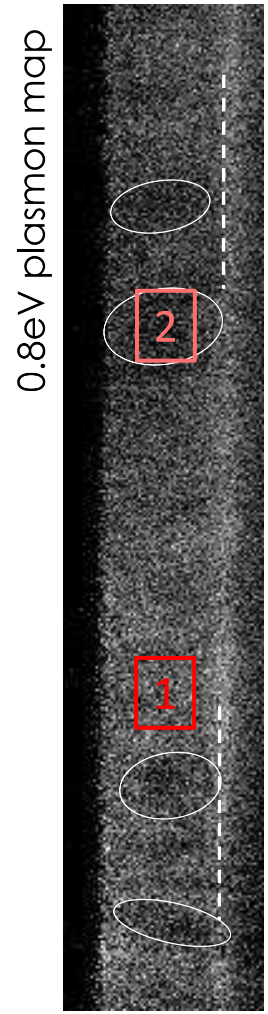

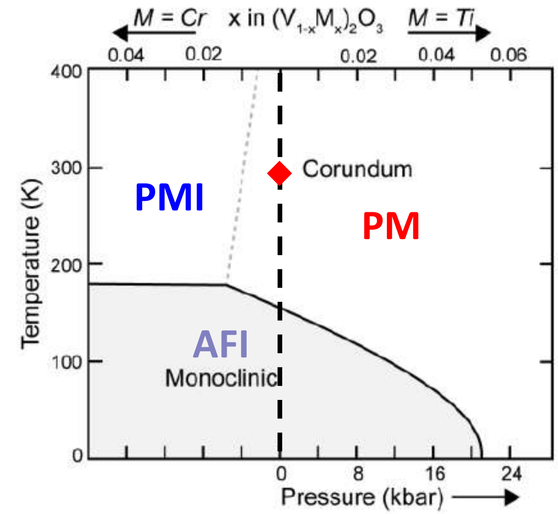

→ local inhomogeneties in the film

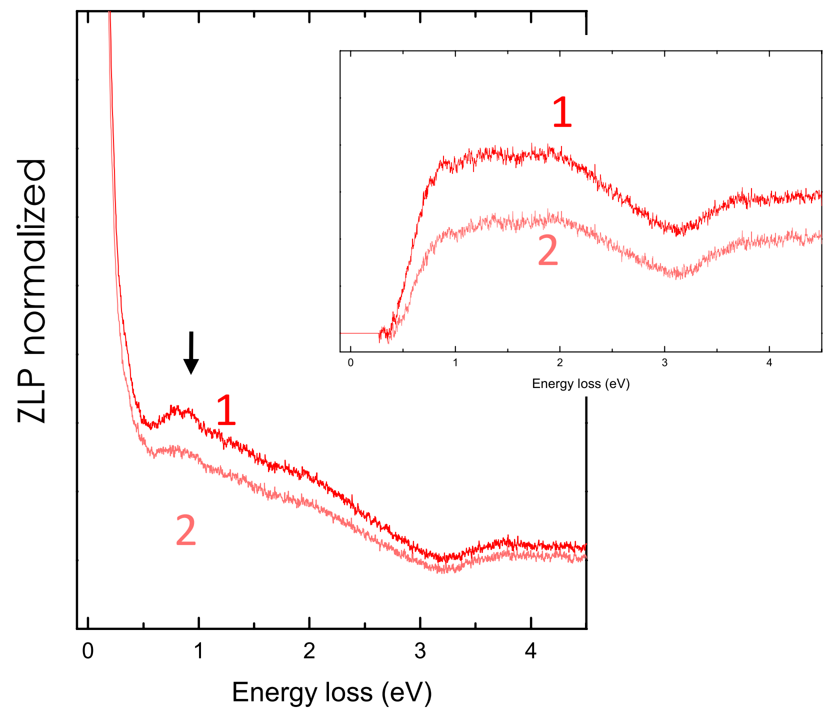

Raw data

- (80x400) px with 12ms/px < 7min in total

L. Bocher, X. Li et al. unpublished

Acknowledgements

STEM group @ LPS-Orsay
https://www.stem.lps.u-psud.fr/

Main collaborators are:

J.M. Triscone et al University of Geneva

V. Garcia, S. Fusil, M. Bibes, A. Barthelemy et al, UMPhy CNRS-Thales

P. van Haken, Max Planck Institute for Solid State Research, Stuttgart

L. Liz-Marzan, CICBiomaGUNE, San Sebastian

A few reviews :

C. Colliex et al., Capturing the signature of single atoms with the tiny probe of a STEM, *Ultramicroscopy*, 123 (2012) 80

A. Gloter et al., Atomically resolved mapping of EELS fine structures, *Materials Science in Semiconductor Processing*, 65 (2017) 2

Stephen J. Pennycook, Peter D. Nellist, Scanning Transmission Electron Microscopy: Imaging and Analysis, Springer Science & Business Media (2011)

ESTEEM 3 in a nutshell

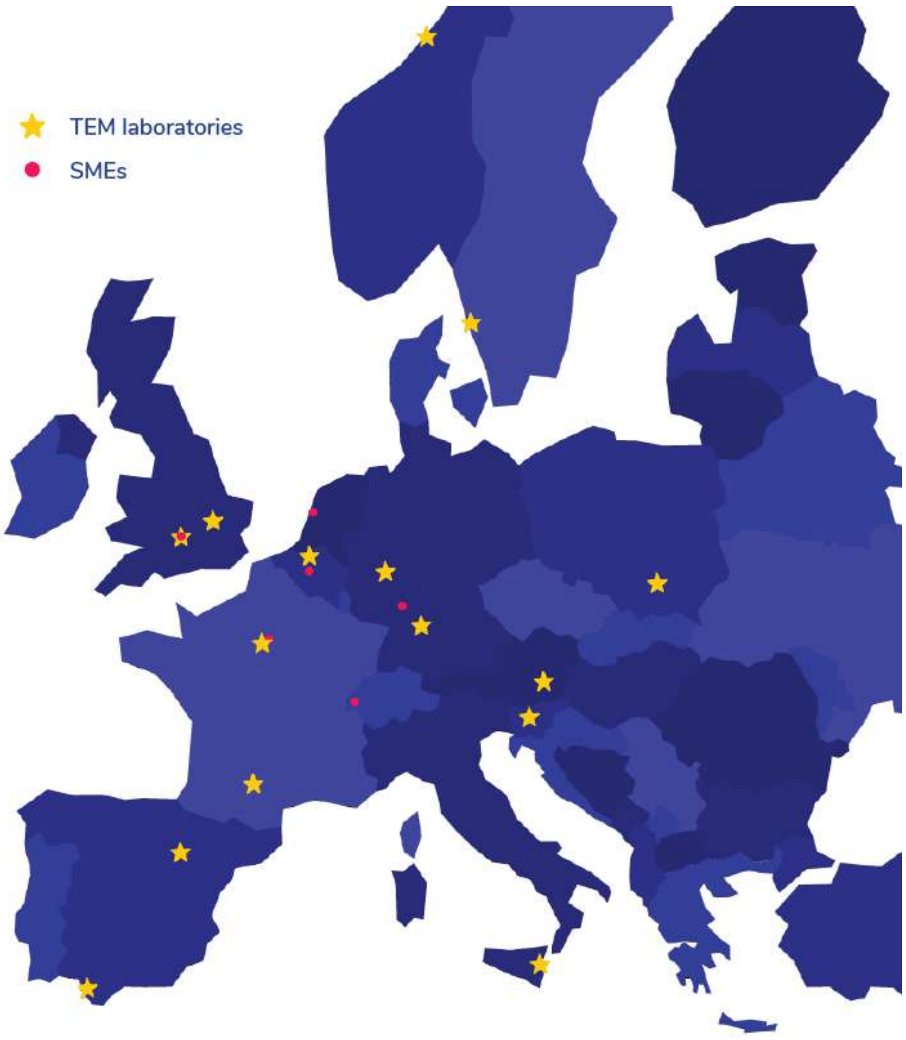

Free transnational access

to the most advanced TEM equipment and skilled operators for HR(S)TEM, EELS, EDX, Tomography, Holography and various in-situ state-of-the-art experiments

Now available to any researcher in the world!

More information at:

esteem3.eu

esteem3@fkf.mpg.de

FR CNRS 3507

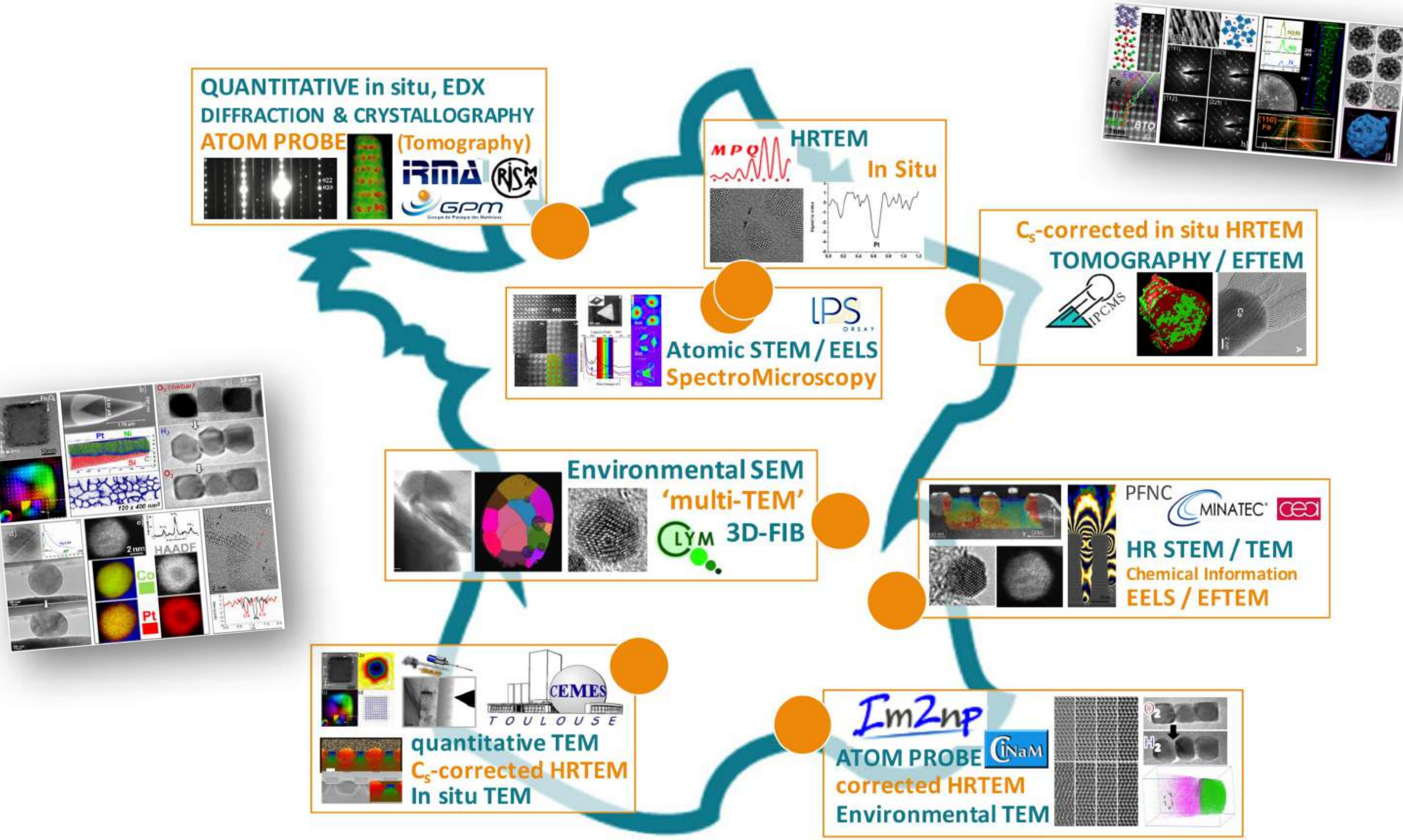
QUANTITATIVE in situ, EDX
DIFFRACTION & CRYSTALLOGRAPHY
ATOM PROBE (Tomography)
RMA
GPM
HRTEM
In Situ
MPQ
C_s-corrected in situ HRTEM
TOMOGRAPHY / EFTEM
IPCMS
LPS ORSAY
Atomic STEM / EELS
SpectroMicroscopy
Environmental SEM
'multi-TEM'
3D-FIB
LYM
PFNC
MINATEC
HR STEM / TEM
Chemical Information
EELS / EFTEM
CEMES
TOULOUSE
quantitative TEM
C_s-corrected HRTEM
In situ TEM
Im2np
CINaM
ATOM PROBE
corrected HRTEM
Environmental TEM